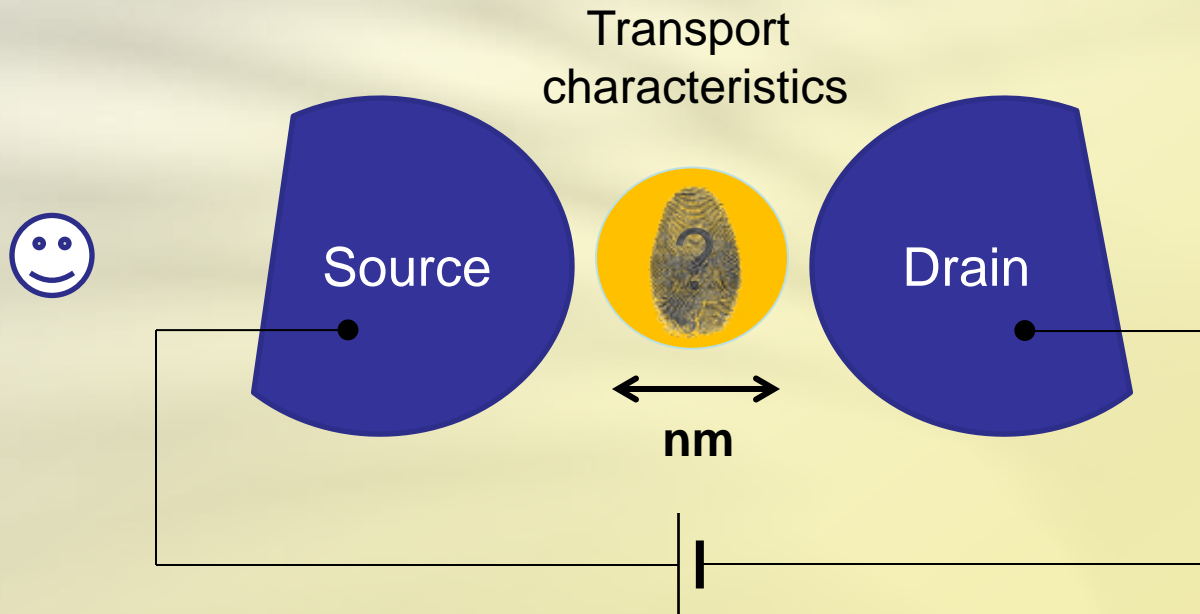


Transport through complex interacting nanojunctions

Andrea Donarini

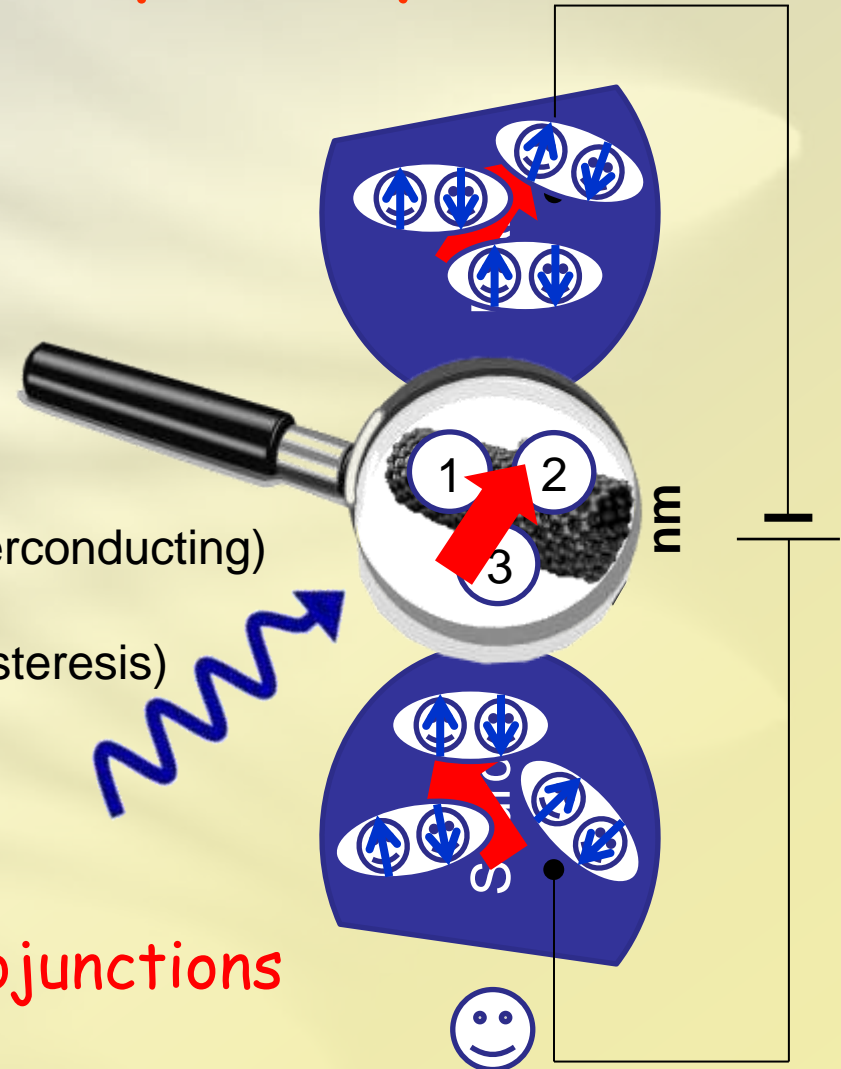


Regensburg - 10.02.2014

Sources of complexity

- Geometry and electronic structure
- Electromechanical interaction
- Spin correlation on the system
- Correlated leads (e.g. ferromagnetic, superconducting)
- Time dependent effects (e.g. switching, hysteresis)
- Interaction with light

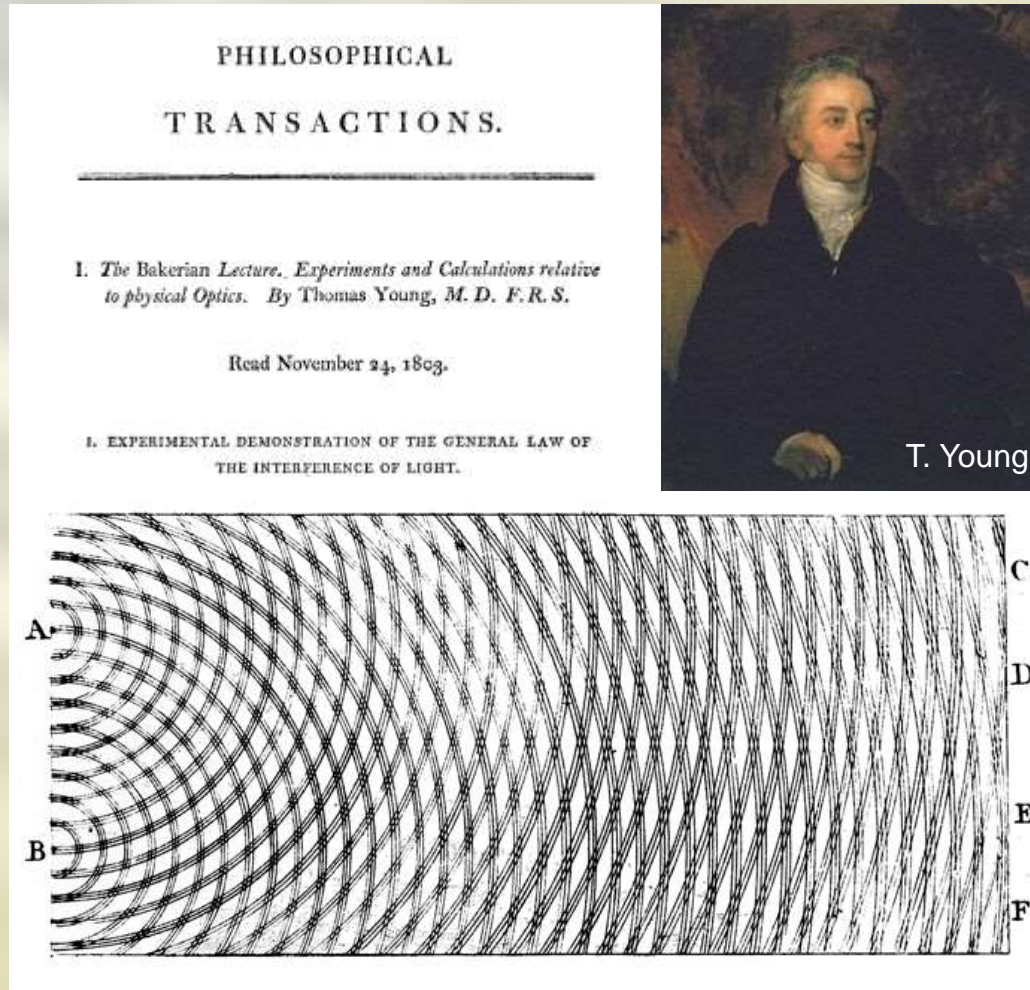
Many-body interference in nanojunctions



Outline

- Brief history of electronic interference
- Interference single electron transistors (I-SET)
- All-electrical spin control in I-SETs
- Topographical fingerprints: STM of Cu-Phthalocyanine
- Conclusions and outlook

Double slit experiment: (London, 1801)



Phil. Trans. R. Soc. Lon., **94**, 12 (1804)

Double slit with electrons: (Tübingen, 1961)

Aus dem Institut für Angewandte Physik der Universität Tübingen

Elektroneninterferenzen an mehreren künstlich hergestellten Feinspalten

Von

CLAUS JÖNSSON

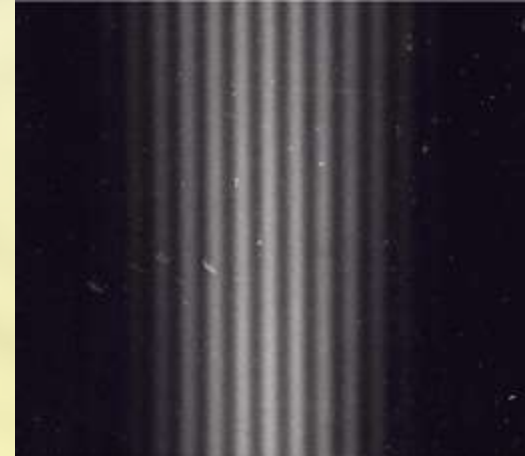
Mit 14 Figuren im Text

(Eingegangen am 17. Oktober 1960)

A glass plate covered with an evaporated silver film of about 200 \AA thickness is irradiated by a line-shaped electron-probe in a vacuum of 10^{-4} Torr. A hydrocarbon polymerisation film of very low electrical conductivity is formed at places subjected to high electron current density. An electrolytically deposited copper film leaves these places free from copper. When the copper film is stripped a grating with slits free of any material is obtained. 50μ long and 0.3μ wide slits with a grating constant of 1μ are obtained. The maximum number of slits is five. The electron diffraction pattern obtained using these slits in an arrangement analogous to Young's light optical interference experiment in the Fraunhofer plane and Fresnel region shows an effect corresponding to the well-known interference phenomena in light optics.



C.Jönsson



Zeitschrift für Physik, **161**, 454 (1961)

Single electron interference (Bologna, 1974)

On the statistical aspect of electron interference phenomena

P. G. Merli

CNR-LAMEL, Bologna, Italy

G. F. Missiroli and G. Pozzi

CNR-GNSM, Istituto di Fisica, Laboratorio Microscopia Elettronica, Bologna, Italy

(Received 29 May 1974; revised 17 October 1974)

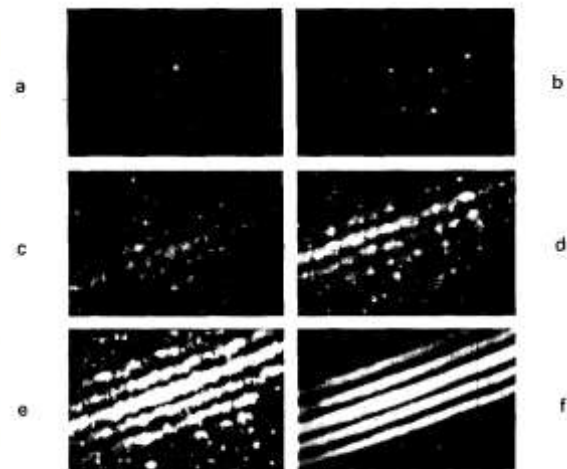


Fig. 1. (a-f) Electron interference fringe patterns filmed from a TV monitor at increasing current densities.

Am. J. Phys., **44**, 306 (1976)

Coherence and Phase Sensitive Measurements in a Quantum Dot

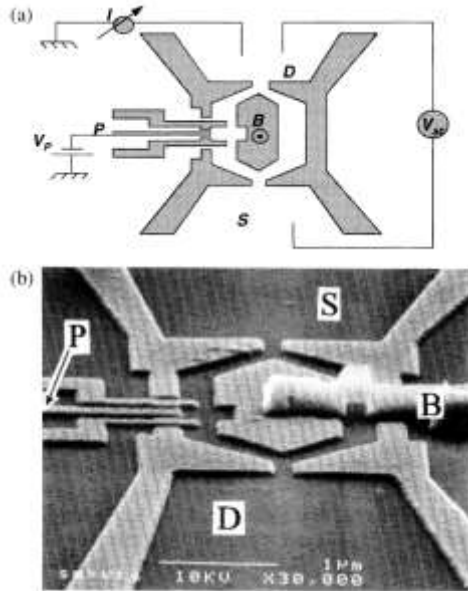
A. Yacoby, M. Heiblum, D. Mahalu, and Hadas Shtrikman

Braun Center for Submicron Research, Department of Condensed Matter Physics, Weizmann Institute of Science, Rehovot 76100, Israel

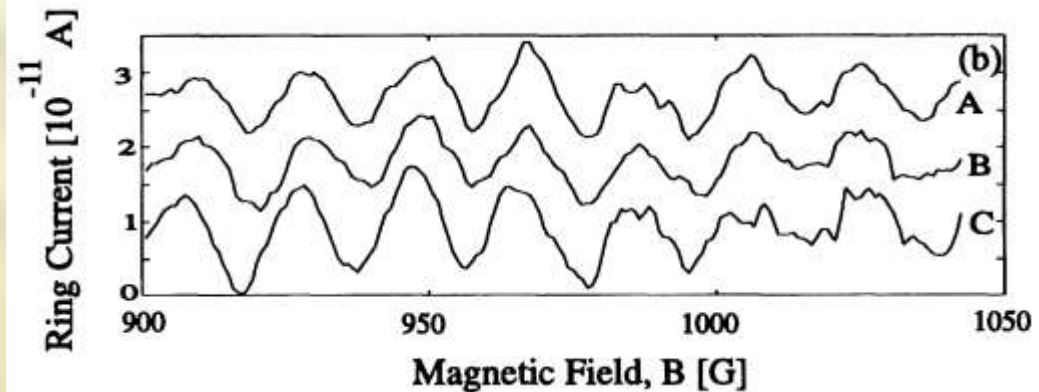
(Received 10 November 1994)

Via a novel interference experiment, which measures magnitude and *phase* of the transmission coefficient through a quantum dot in the Coulomb regime, we prove directly, for the first time, that transport through the dot has a coherent component. We find the same phase of the transmission coefficient at successive Coulomb peaks, each representing a different number of electrons in the dot; however, as we scan through a single Coulomb peak we find an *abrupt* phase change of π . The observed behavior of the phase cannot be understood in the single particle framework.

PACS numbers: 73.20.Dx, 71.45.-d, 72.80.Ey, 73.40.Gk



M. Heiblum

*Phys. Rev. Lett.*, **74**, 4047 (1995)

...counting single electrons (Zürich, 2008)

NANO
LETTERS

2008
Vol. 8, No. 8
2547-2550

Time-Resolved Detection of Single-Electron Interference

S. Gustavsson,^{*} R. Leturcq, M. Studer, T. Ihn, and K. Ensslin

Solid State Physics Laboratory, ETH Zürich, CH-8093 Zürich, Switzerland

D. C. Driscoll and A. C. Gossard

Materials Department, University of California, Santa Barbara, California 93106

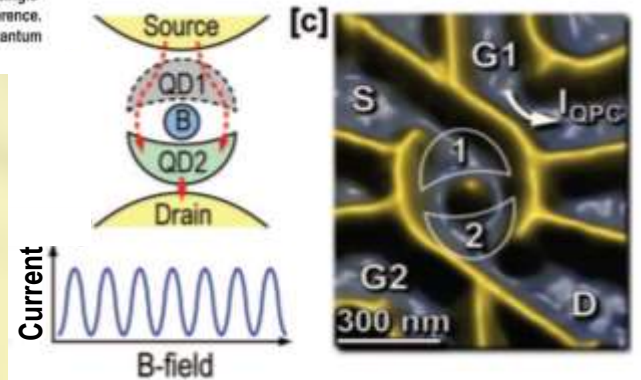
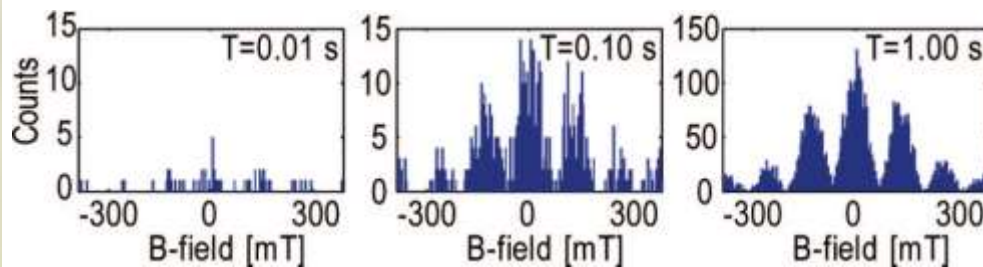
Received June 13, 2008

ABSTRACT

We demonstrate real-time detection of self-interfering electrons in a double quantum dot embedded in an Aharonov–Bohm interferometer, with visibility approaching unity. We use a quantum point contact as a charge detector to perform time-resolved measurements of single-electron tunneling. With increased bias voltage, the quantum point contact exerts a back-action on the interferometer leading to decoherence. We attribute this to emission of radiation from the quantum point contact, which drives noncoherent electronic transitions in the quantum dots.

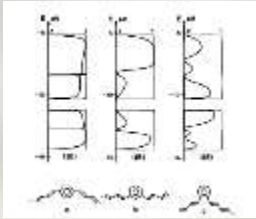


K. Ensslin

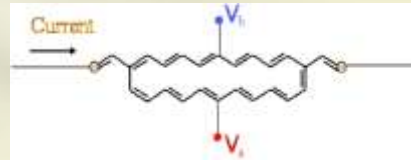


Nano Lett., **8**, 2547 (2008)

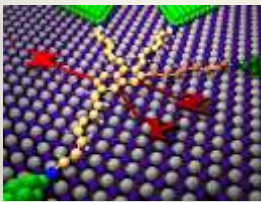
Intramolecular interference: theoretical proposals



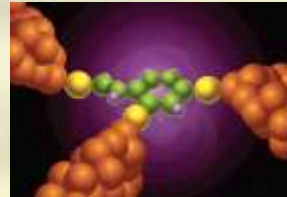
P. Sautet and C. Joachim
Chem. Phys. Lett. **153**, 511 (1988)



R. Baer and D. Neuhauser
JACS, **124**, 4200 (2002)



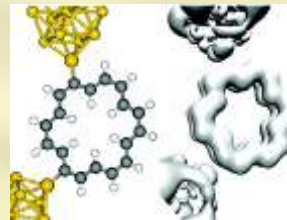
R. Stadler, et al.
Nanotechnology, **14**, 138 (2003)



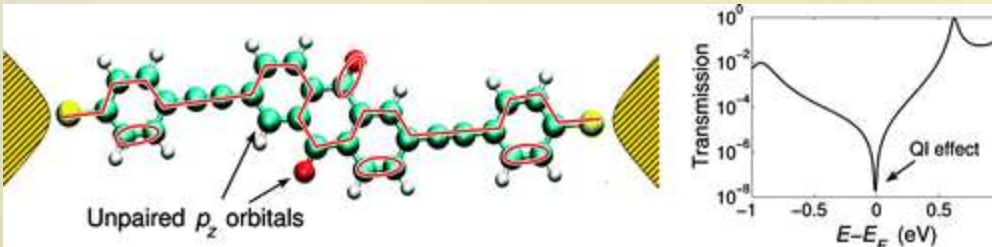
D. V. Cardamone, et al.
Nano Lett., **6**, 2422 (2006)



G. Solomon, et al.
JACS **130**, 17307 (2008)

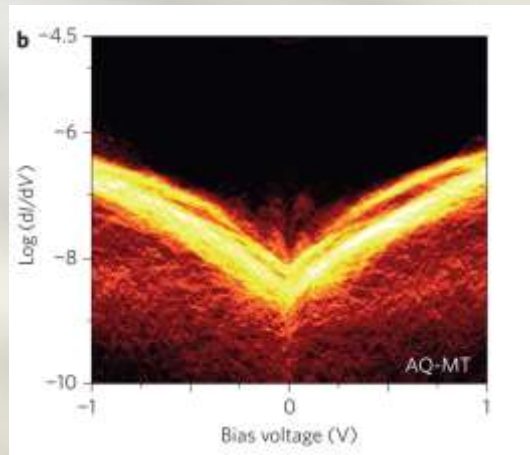


S.H. Ke, et al.
Nano Lett., **8**, 3257 (2008)

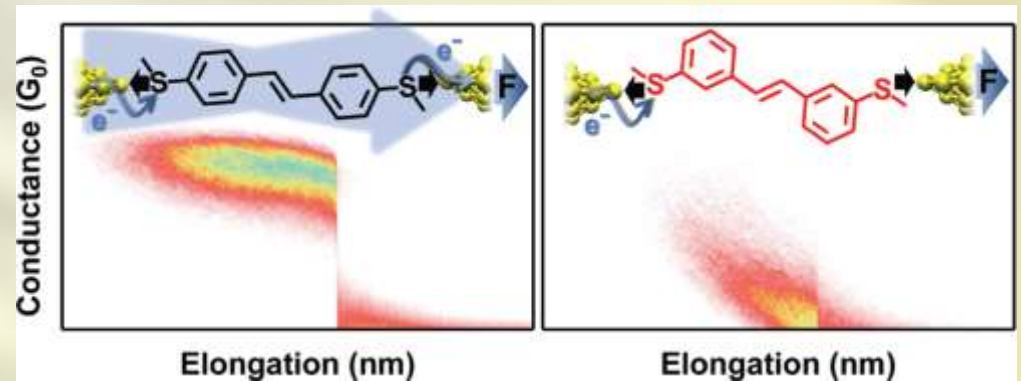


T. Markussen, et al.
Nano Lett., **10**, 4260 (2010)

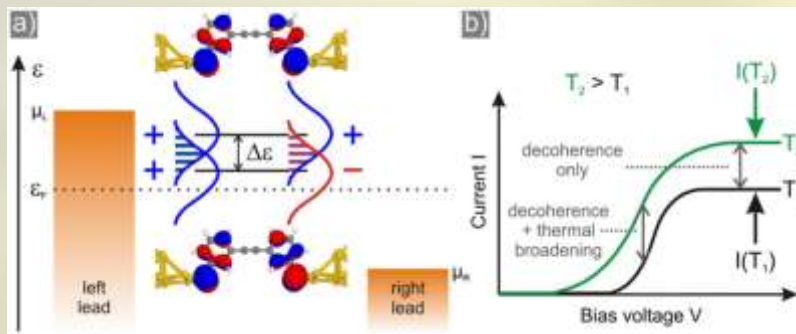
Experimental evidence



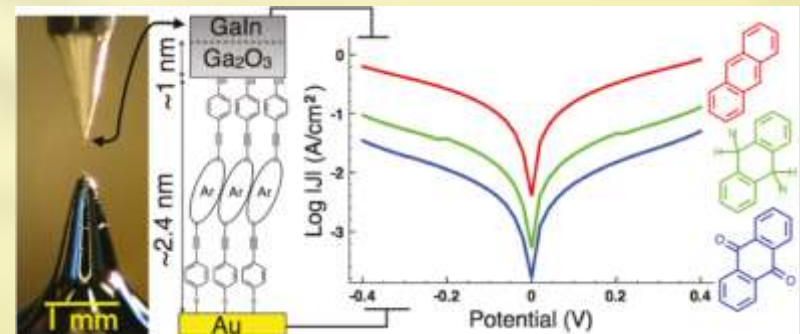
Guédon et al. *Nature Nanotech.* **7**, 305 (2012)



Aradhya et al. *Nano Lett.*, **12**, 1643 (2012)

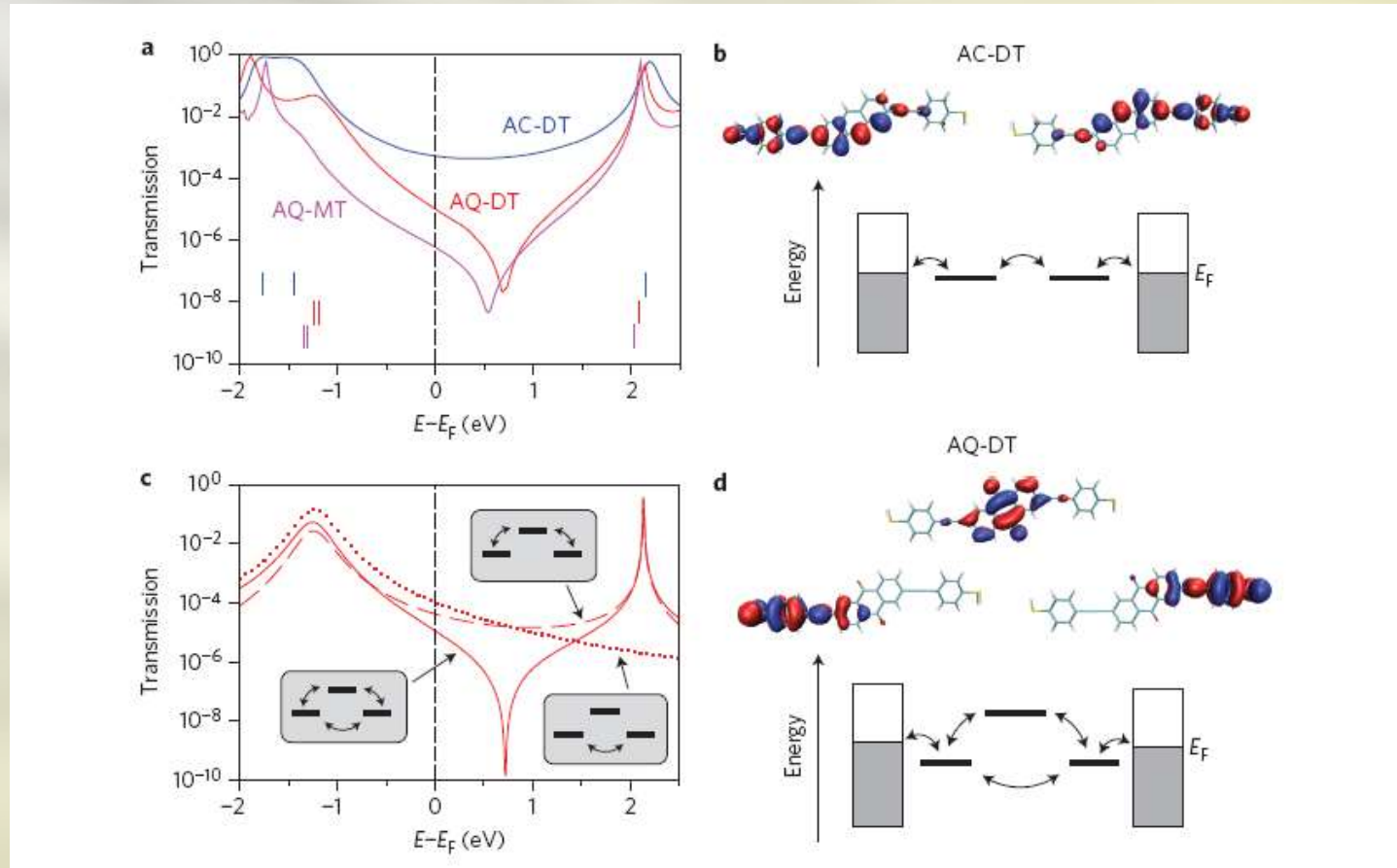


Ballman et al. *PRL* **109**, 056801 (2012)



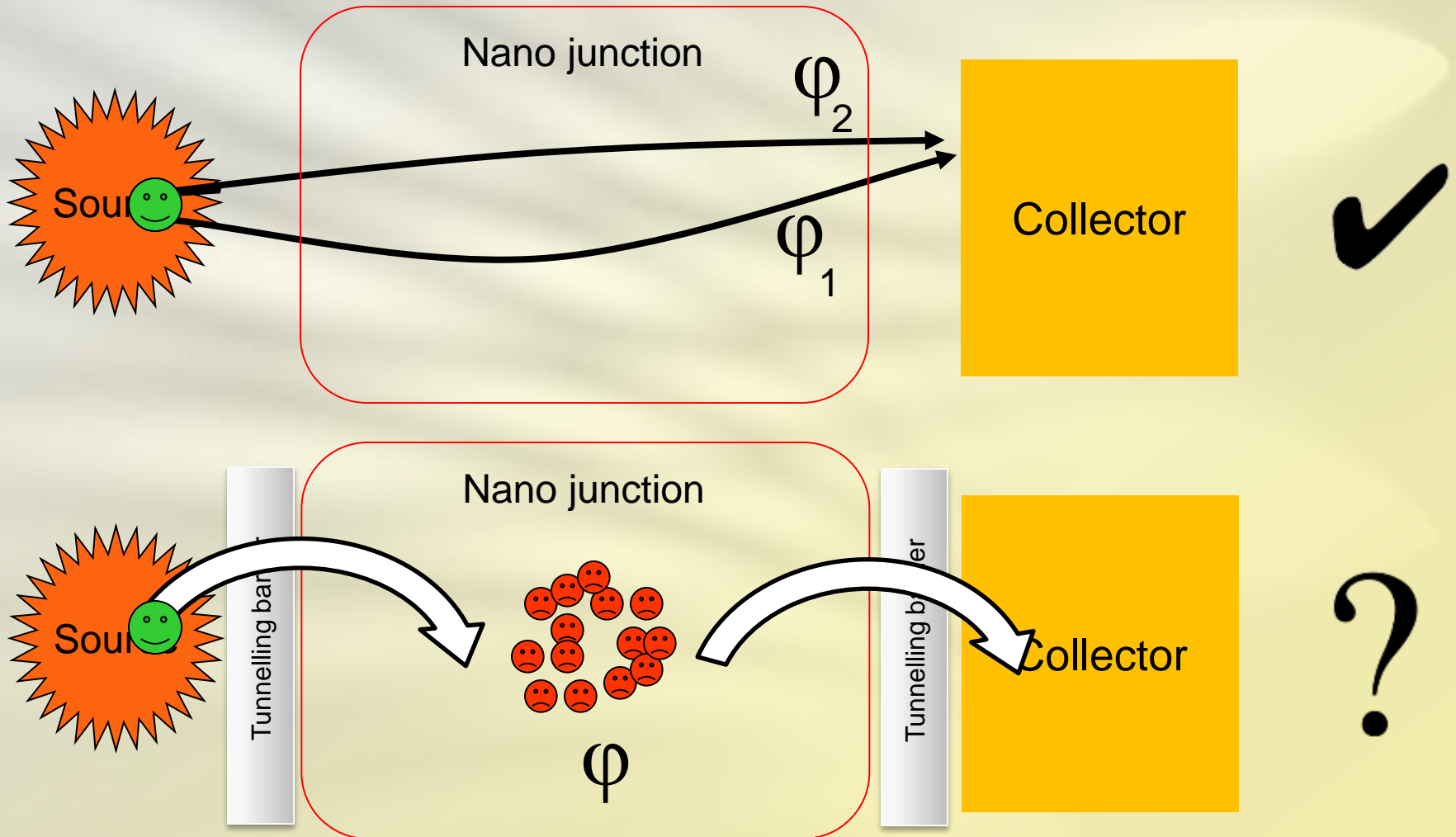
Fracasso et al. *JACS*, **133**, 9556 (2011)

Destructive interference

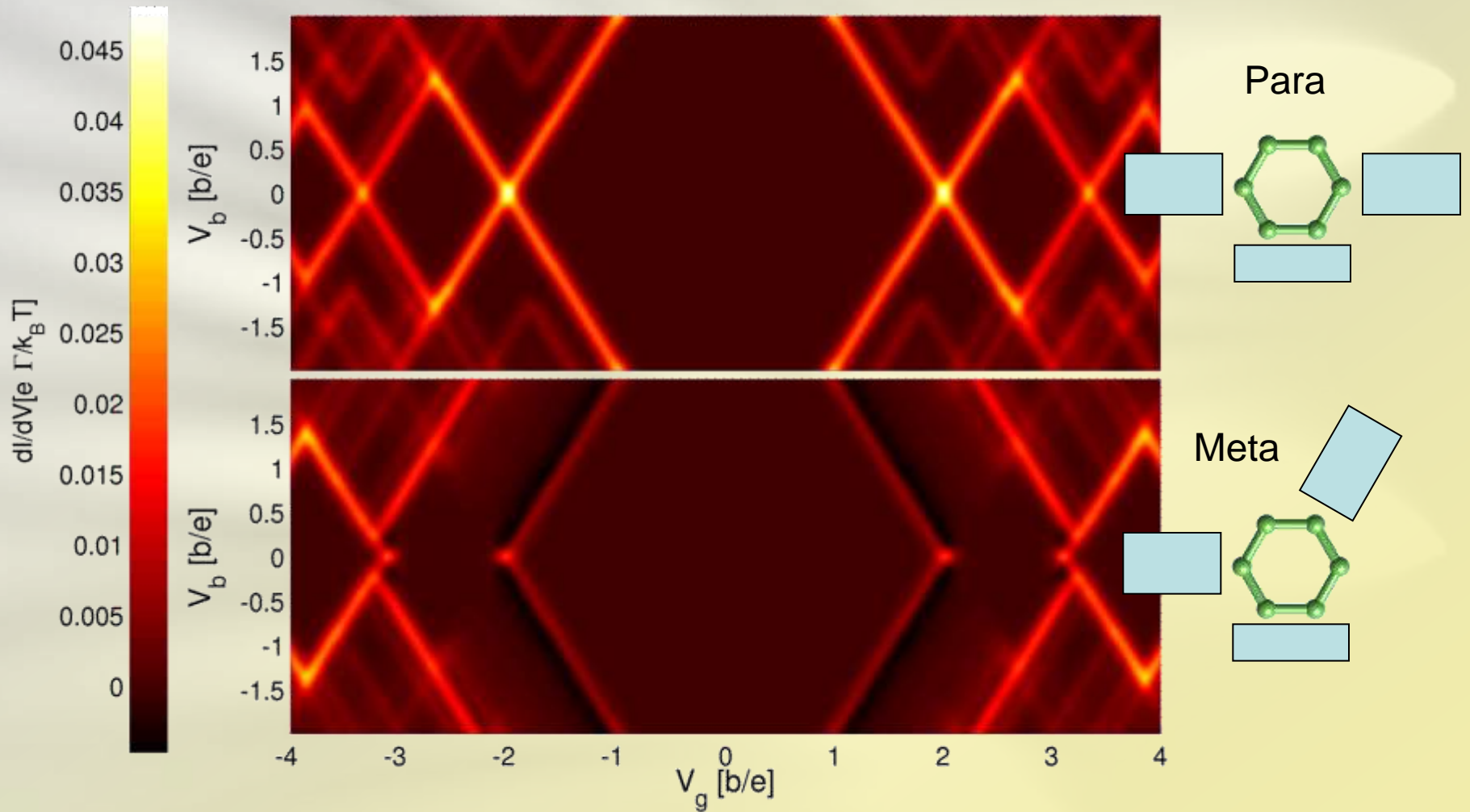


C. M. Guédon, H. Valkenier et al. *Nature Nanotech.* **7**, 305 (2012)

Interference and dephasing



Interference in weak coupling



G. Begemann, D. Darau, **AD**, M. Grifoni, *Phys. Rev. B* **77**, 201406(R) (2008)

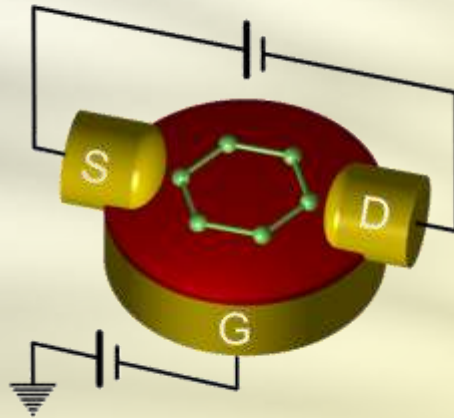
Regensburg - 10.02.2014

physikalisches

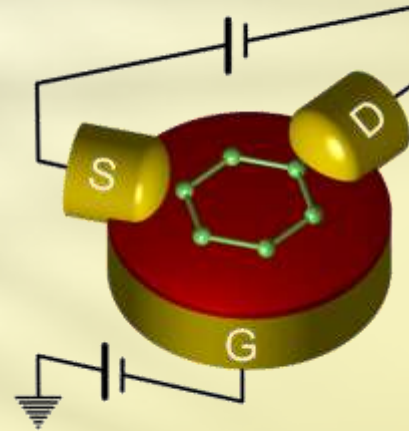
Interference

Single Electron Transistors

PARA configuration



META configuration



G. Begemann, D. Darau, **AD**, M. Grifoni, *Phys. Rev. B* **77**, 201406(R) (2008)

D. Darau, G. Begemann, **AD**, M. Grifoni, *Phys. Rev. B* **79**, 235404 (2009)

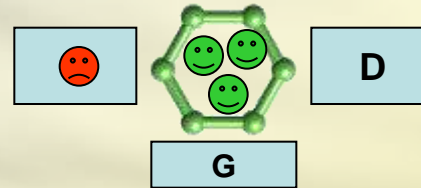
AD, M. Grifoni, Ch.7 of the book "Quantum Dot Molecules", Springer (2014)

(Benzene) ISET...

- **Weak coupling**
- **Coulomb** interaction
- Molecular **size**
- **Low** temperature



Coulomb blockade

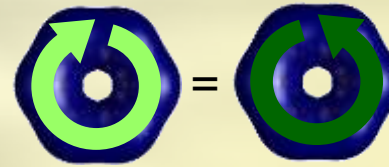


$$\hbar\Gamma \ll k_B T \ll \Delta E_{ex}$$

- **Rotational** symmetry



Orbitally degenerate states

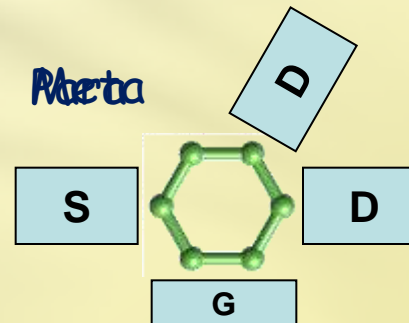


$$E_1 = E_2$$

- Contact **geometry**

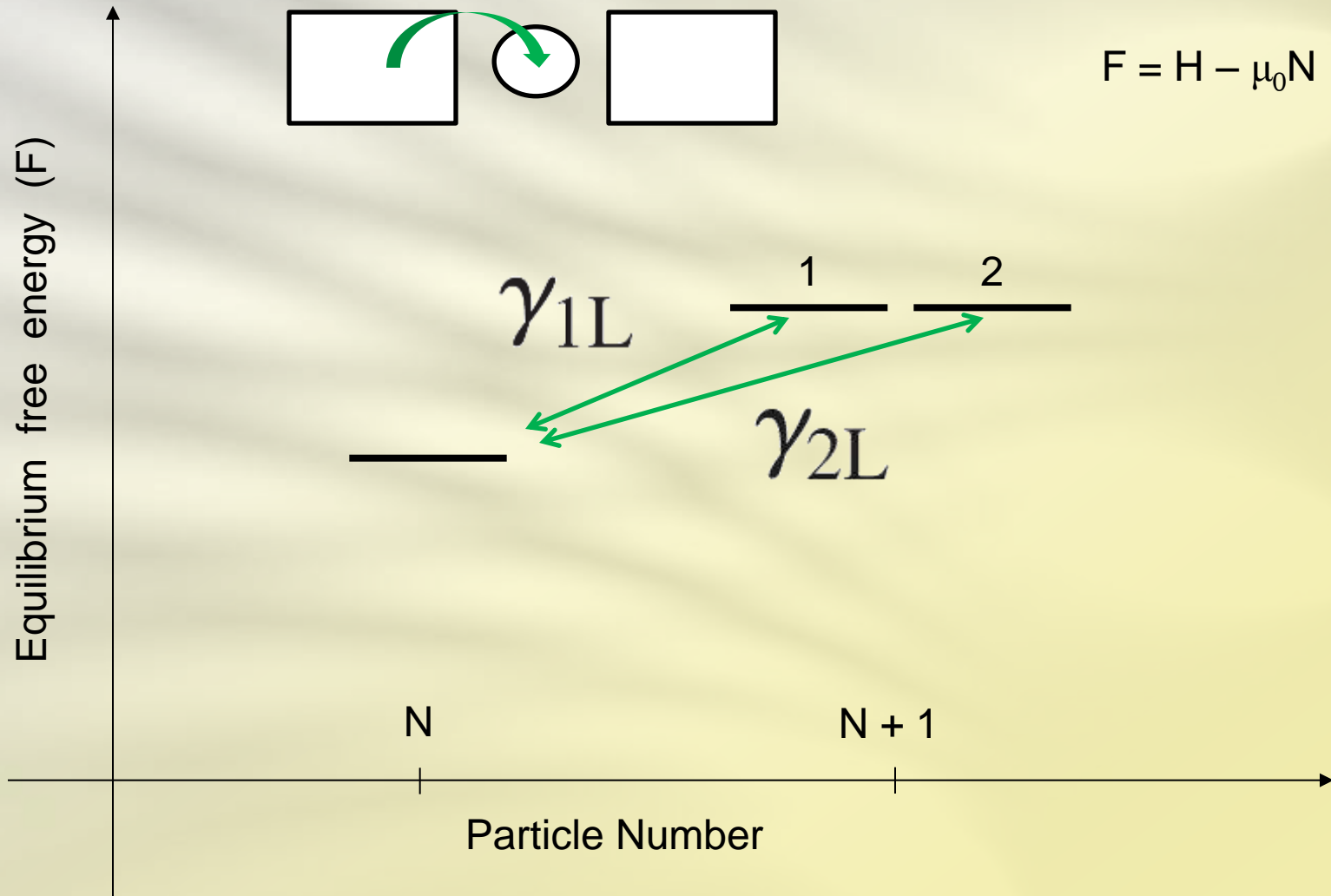


Contact symmetry breaking

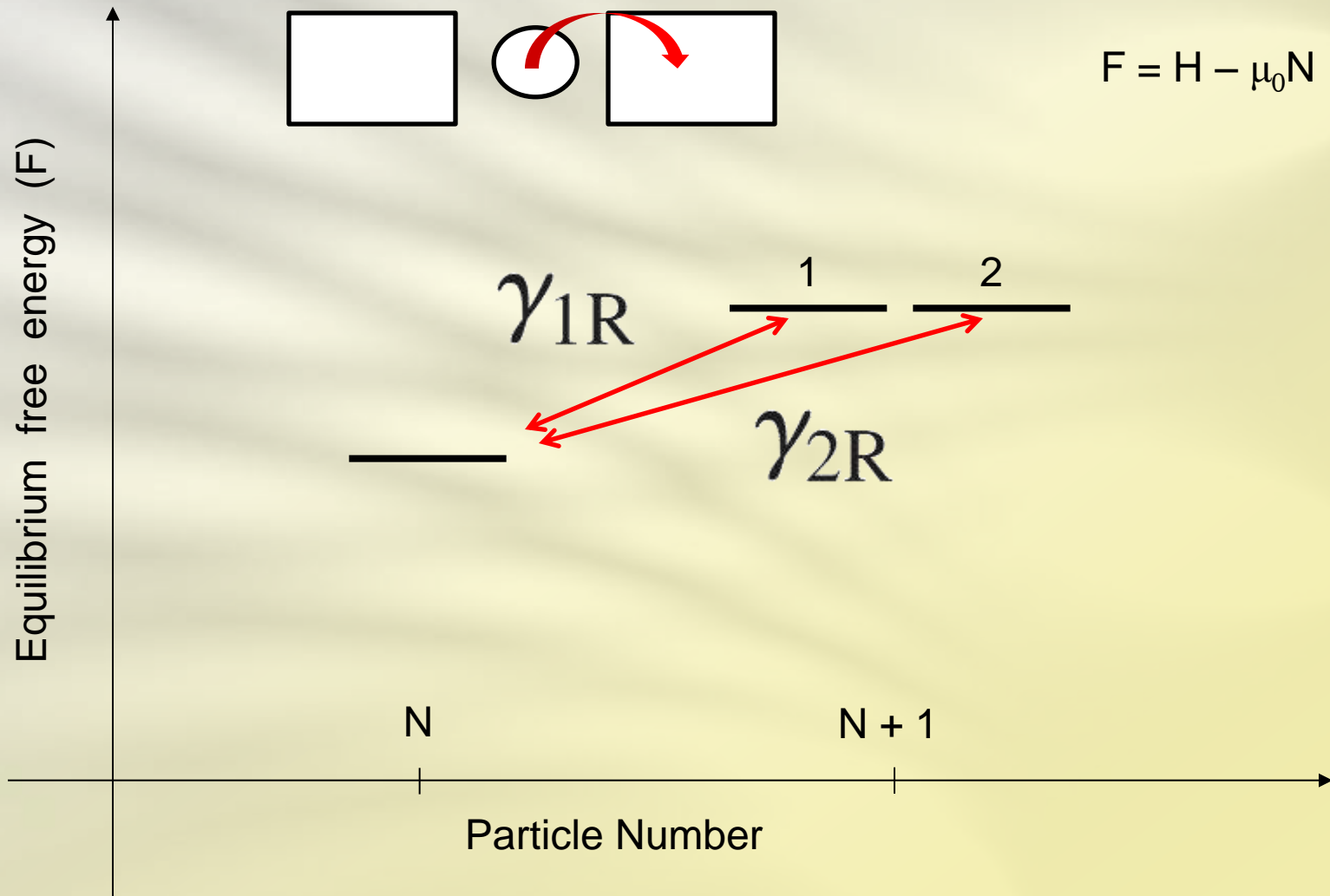


$$\frac{\gamma_{1L}}{\gamma_{2L}} \neq \frac{\gamma_{1R}}{\gamma_{2R}}$$

Many-body tunnelling amplitudes



Many-body tunnelling amplitudes



Contact symmetry breaking

$$|1'\rangle = a|1\rangle + b|2\rangle \quad \Rightarrow \quad \gamma_{1'L} = a\gamma_{1L} + b\gamma_{2L}$$

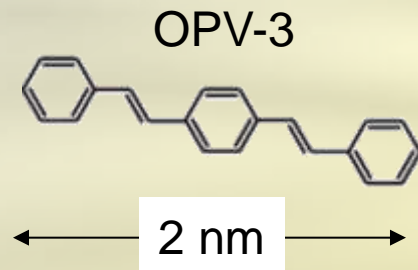
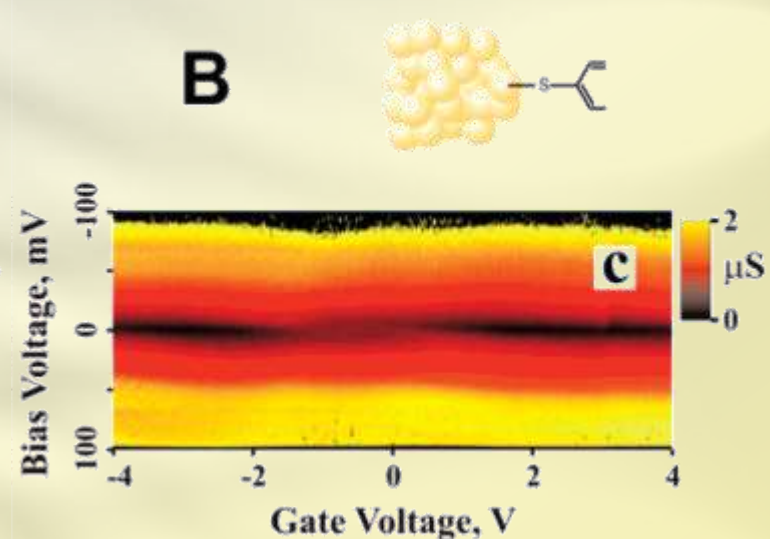
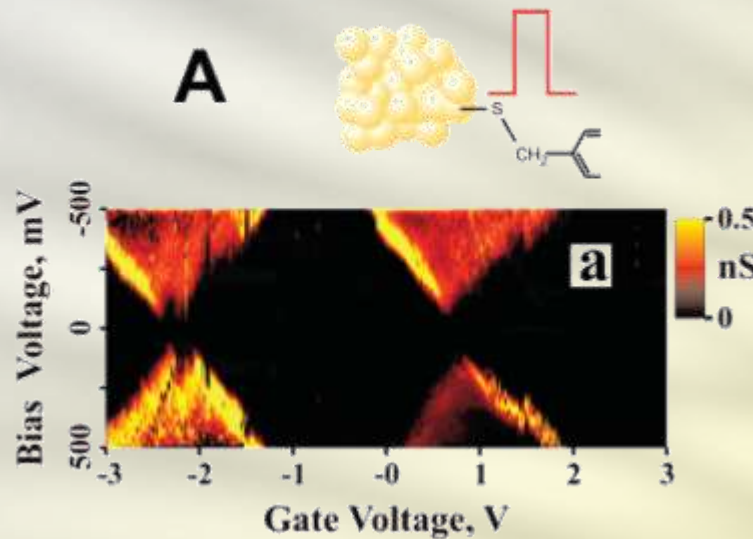
$$\boxed{\frac{\gamma_{1L}}{\gamma_{2L}} \neq \frac{\gamma_{1R}}{\gamma_{2R}}} \quad \Rightarrow \quad \exists \begin{array}{l} |1'\rangle \\ |2'\rangle \end{array} \quad \begin{array}{l} \gamma_{1'L} \neq 0 \\ \gamma_{1'R} = 0 \\ \gamma_{2'L} \neq 0 \\ \gamma_{2'R} \neq 0 \end{array}$$

More degenerate states? See

AD, G. Begemann and M. Grifoni *Phys. Rev. B*, **82**, 125451 (2010)

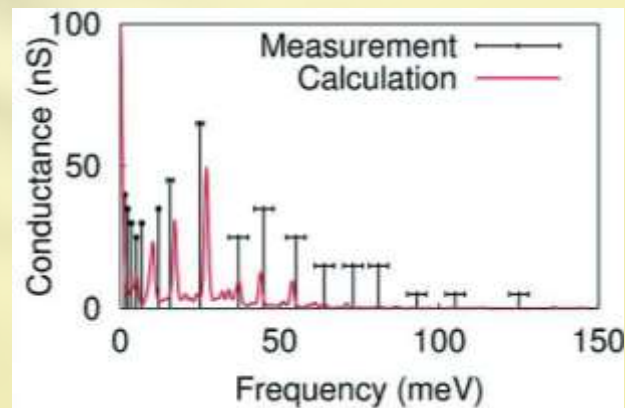
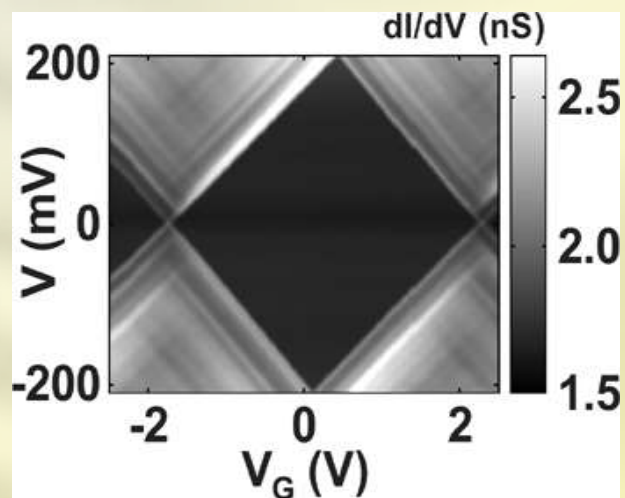
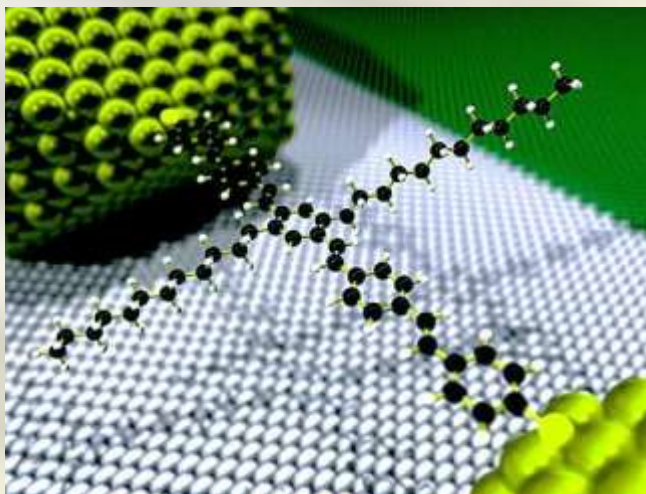
for the general theory.

The coupling strength



- **Gating** of 2 nm sized molecule
- **Weak coupling** realization with specific anchor groups

Single molecule SET

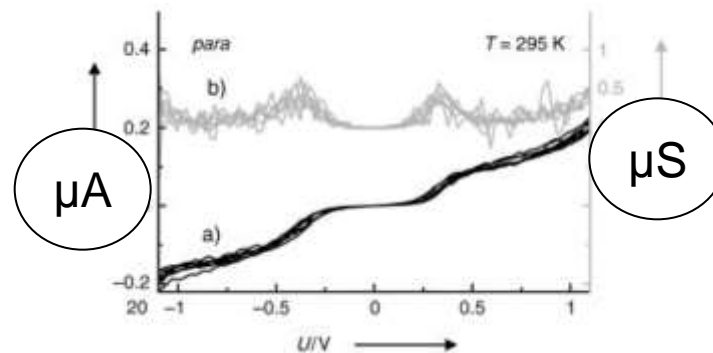
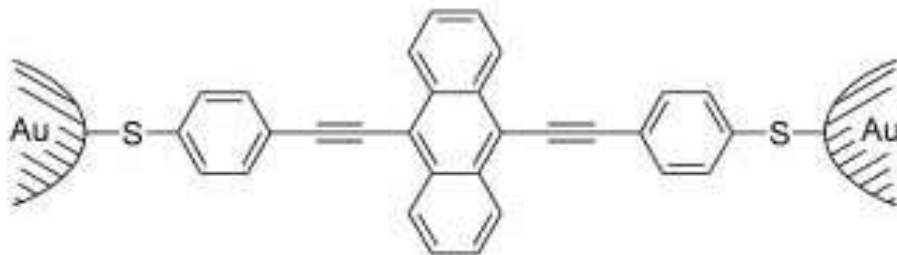


E. A. Osorio et al., *Advanced Materials* **19**, 281 (2007)

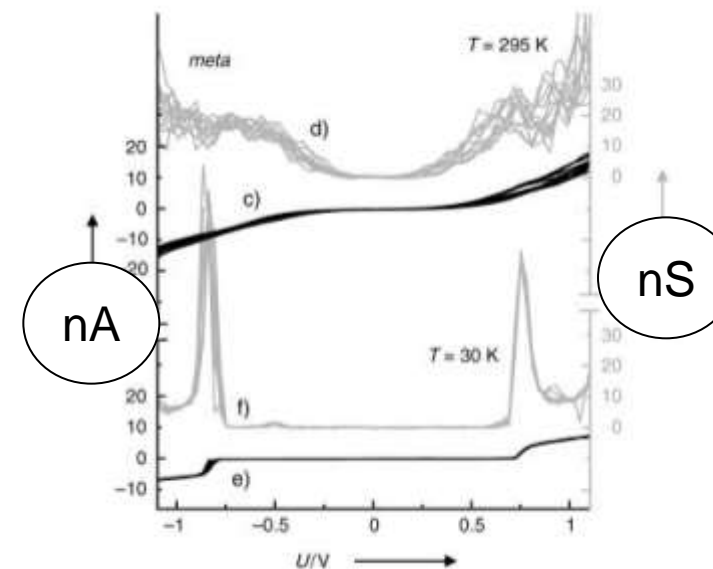
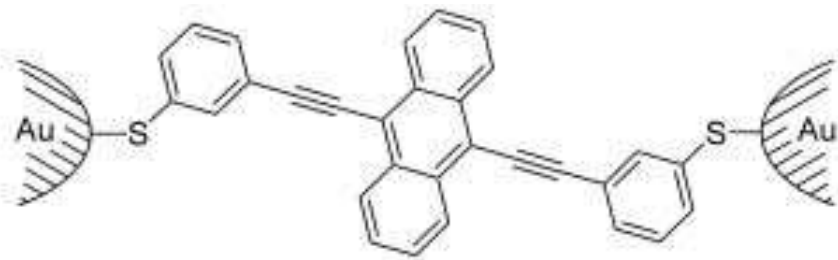
J. S. Seldenthuis et al., *ACS Nano* **2**, 1445 (2008)

The contact geometry

Para configuration



Meta configuration

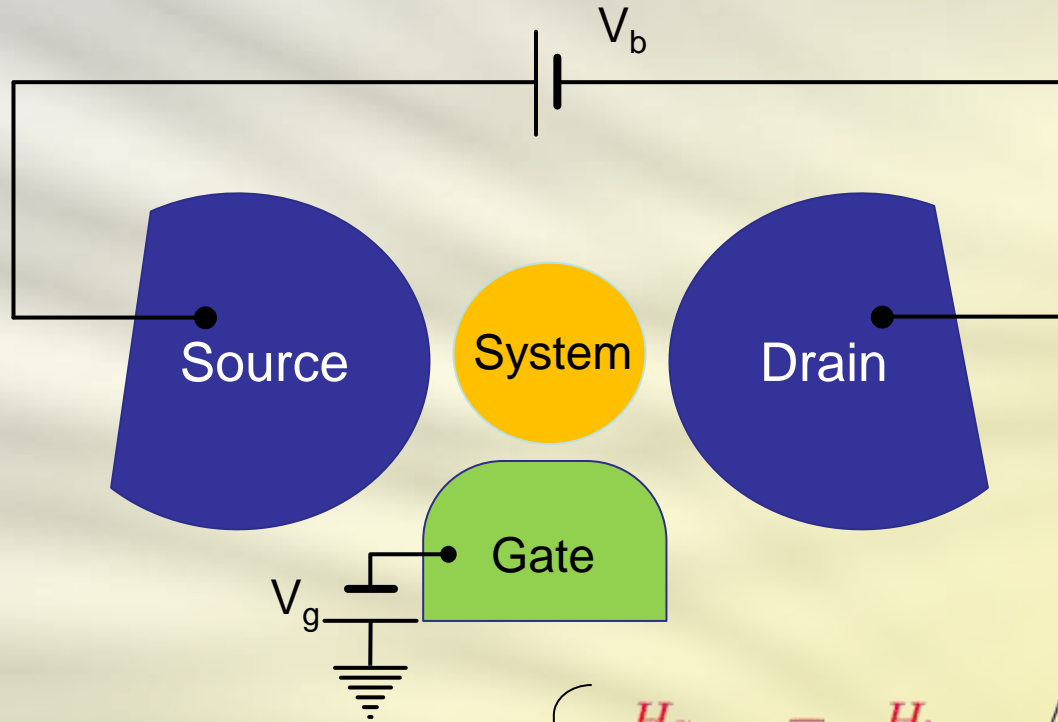


M. Mayor, H. Weber, et al. *Angew. Chem. Int. Ed.* **42** 5843 (2003)

Regensburg - 10.02.2014

physikalisches

The Hamiltonian

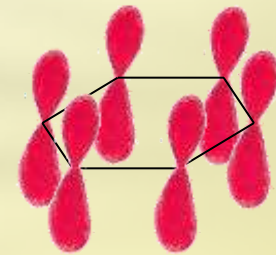


$$H = H_{\text{Sys}} + H_{\text{leads}} + H_{\text{tun}} \left\{ \begin{array}{l} H_{\text{Sys}} = H_{\text{ben}} / H_{\text{TD}} \\ H_{\text{leads}} = \sum_{\alpha k \sigma} \epsilon_k c_{\alpha k \sigma}^\dagger c_{\alpha k \sigma} \\ H_{\text{tun}} = t \sum_{\alpha k \sigma} \left(d_{\alpha \sigma}^\dagger c_{\alpha k \sigma} + c_{\alpha k \sigma}^\dagger d_{\alpha \sigma} \right) \end{array} \right.$$

Interacting isolated benzene

- The **Pariser-Parr-Pople** Hamiltonian for isolated benzene reads:

$$\begin{aligned}
 H_{\text{ben}}^0 &= \xi_0 \sum_{i\sigma} d_{i\sigma}^\dagger d_{i\sigma} + b \sum_{i\sigma} \left(d_{i\sigma}^\dagger d_{i+1\sigma} + d_{i+1\sigma}^\dagger d_{i\sigma} \right) \\
 &+ U \sum_i \left(n_{i\uparrow} - \frac{1}{2} \right) \left(n_{i\downarrow} - \frac{1}{2} \right) \\
 &+ V \sum_i \left(n_{i\uparrow} + n_{i\downarrow} - 1 \right) \left(n_{i+1\uparrow} + n_{i+1\downarrow} - 1 \right)
 \end{aligned}$$



- The **size** of the Fock space for the many-body system $4^6 = 4096$ since for each site there are 4 possibilities: $|0\rangle, |\uparrow\rangle, |\downarrow\rangle, |\uparrow\downarrow\rangle$
- Within this Fock space we diagonalize **exactly** the Hamiltonian.

Symmetry of the ground states

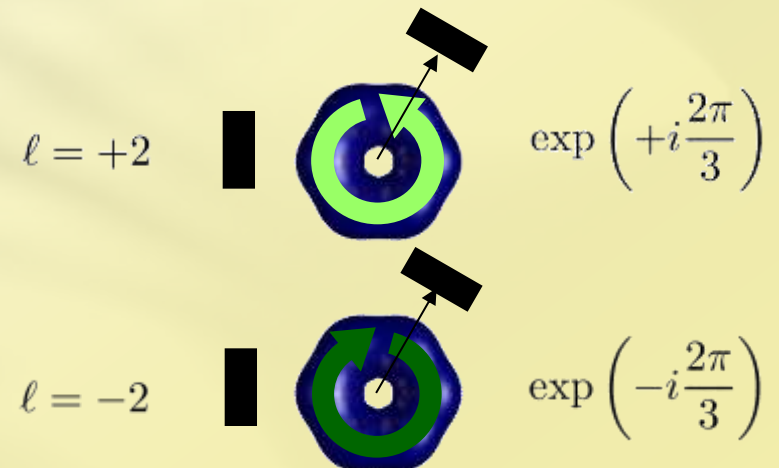
N	Degeneracy	GS energy[eV] (at $\xi = 0$)	GS symmetry representation
0	1	0	A_{1g}
1	2	-22	A_{2u}
2	1	-42.25	A_{1g}
3	4	-57.42	E_{1g}
4	3	-68.875	A_{2g}
5	4	-76.675	E_{1g}
6	1	-81.725	A_{1g}
7	4	-76.675	E_{2u}
8	3	-68.875	A_{2g}
9	4	-57.42	E_{2u}
10	1	-42.25	A_{1g}
11	2	-22	B_{2g}
12	1	0	A_{1g}

Rotation phase factors

Under rotation of an angle $\phi = \frac{n\pi}{3}$

- $\mathcal{R}_\phi |6_g\rangle = |6_g\rangle$ No phase acquired


- $\mathcal{R}_\phi |7_g \ell\rangle = e^{-i\ell\phi} |7_g \ell\rangle$ $\ell = \pm 2$



Generalized Master Equation

- We start with the **Liouville** equation: $\dot{\rho} = -\frac{i}{\hbar}[\mathcal{H}, \rho]$

- We define the reduced density matrix $\sigma = \text{Tr}_{\text{Leads}}\{\rho\}$ which is **block-diagonal** in

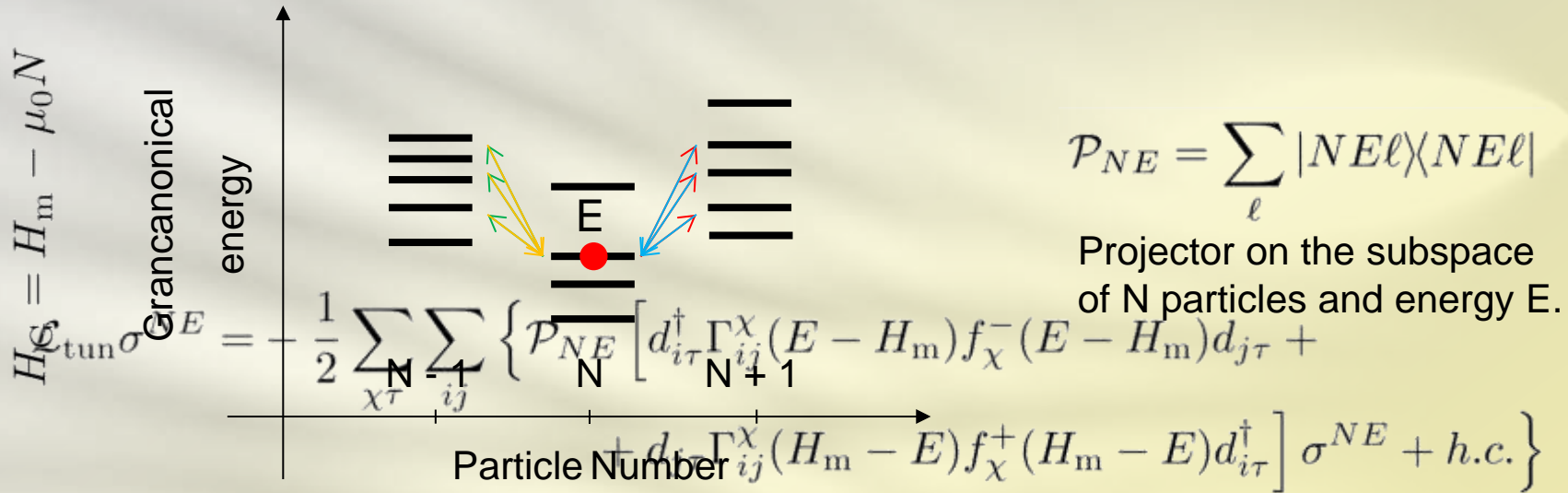
$$\sigma =$$


particle number
spin
energy

- We keep the coherences between **orbitally** degenerate states.
- The **Generalized Master Equation** is the equation of motion for σ :

$$\dot{\sigma} = \underbrace{-\frac{i}{\hbar}[H_{\text{sys}}, \sigma]}_{\text{Coherent dynamics}} - \underbrace{\frac{i}{\hbar}[H_{\text{eff}}, \sigma]}_{\text{Effective internal dynamics}} + \underbrace{\mathcal{L}_{\text{tun}}\sigma}_{\text{Tunnelling dynamics}}$$

Tunnelling Liouvillean



$$\mathcal{P}_{NE} = \sum_{\ell} |NE\ell\rangle\langle NE\ell|$$

Projector on the subspace of N particles and energy E.

$$+ \sum_{\chi\tau} \sum_{ijE'} \mathcal{P}_{NE} \left[d_{i\tau}^\dagger \Gamma_{ij}^\chi (E - E') \sigma^{N-1E'} f_\chi^+(E - E') d_{j\tau} + \right.$$

$$\left. + d_{j\tau} \Gamma_{ij}^\chi (E' - E) \sigma^{N+1E'} f_\chi^-(E' - E) d_{i\tau}^\dagger \right] \mathcal{P}_{NE}$$

Single particle rate matrix

$$\Gamma_{ij}^{\chi}(\Delta E) = \frac{2\pi}{\hbar} \sum_k (t_{ki}^{\chi})^* t_{kj}^{\chi} \delta(\varepsilon_k^{\chi} - \Delta E)$$

$$H_{\text{eff}} = \frac{1}{2\pi} \sum_{NE} \sum_{\chi\sigma} \sum_{ij} \mathcal{P}_{NE} \left[d_{i\sigma}^{\dagger} \Gamma_{ij}^{\chi}(E - H_m) p_{\chi}(E - H_m) d_{j\sigma} \right. \\ \left. + d_{j\sigma} \Gamma_{ij}^{\chi}(H_m - E) p_{\chi}(H_m - E) d_{i\sigma}^{\dagger} \right] \mathcal{P}_{NE}$$

Effective
Hamiltonian

$$I_{\chi} = \sum_{NE\sigma ij} \mathcal{P}_{NE} \left[d_{j\sigma} \Gamma_{ij}^{\chi}(H_m - E) f_{\chi}^{+}(H_m - E) d_{i\sigma}^{\dagger} \right. \\ \left. - d_{i\sigma}^{\dagger} \Gamma_{ij}^{\chi}(E - H_m) f_{\chi}^{-}(E - H_m) d_{j\sigma} \right] \mathcal{P}_{NE}$$

Current
operator

Many-body rate matrix

The **current** is proportional to the **transition rate** between **many-body states**

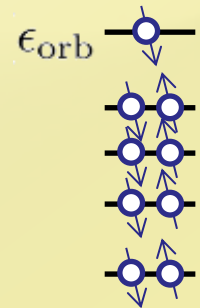
$$R_{N E_0 \rightarrow N+1 E_1}^{X\tau} = \sum_{ij} \langle N+1 E_1 | d_{i\tau}^\dagger | N E_0 \rangle \Gamma_{ij}^X(E_1 - E_0) \times \\ \langle N E_0 | d_{j\tau} | N+1 E_1 \rangle f^+(E_1 - E_0 - \mu_X)$$

where

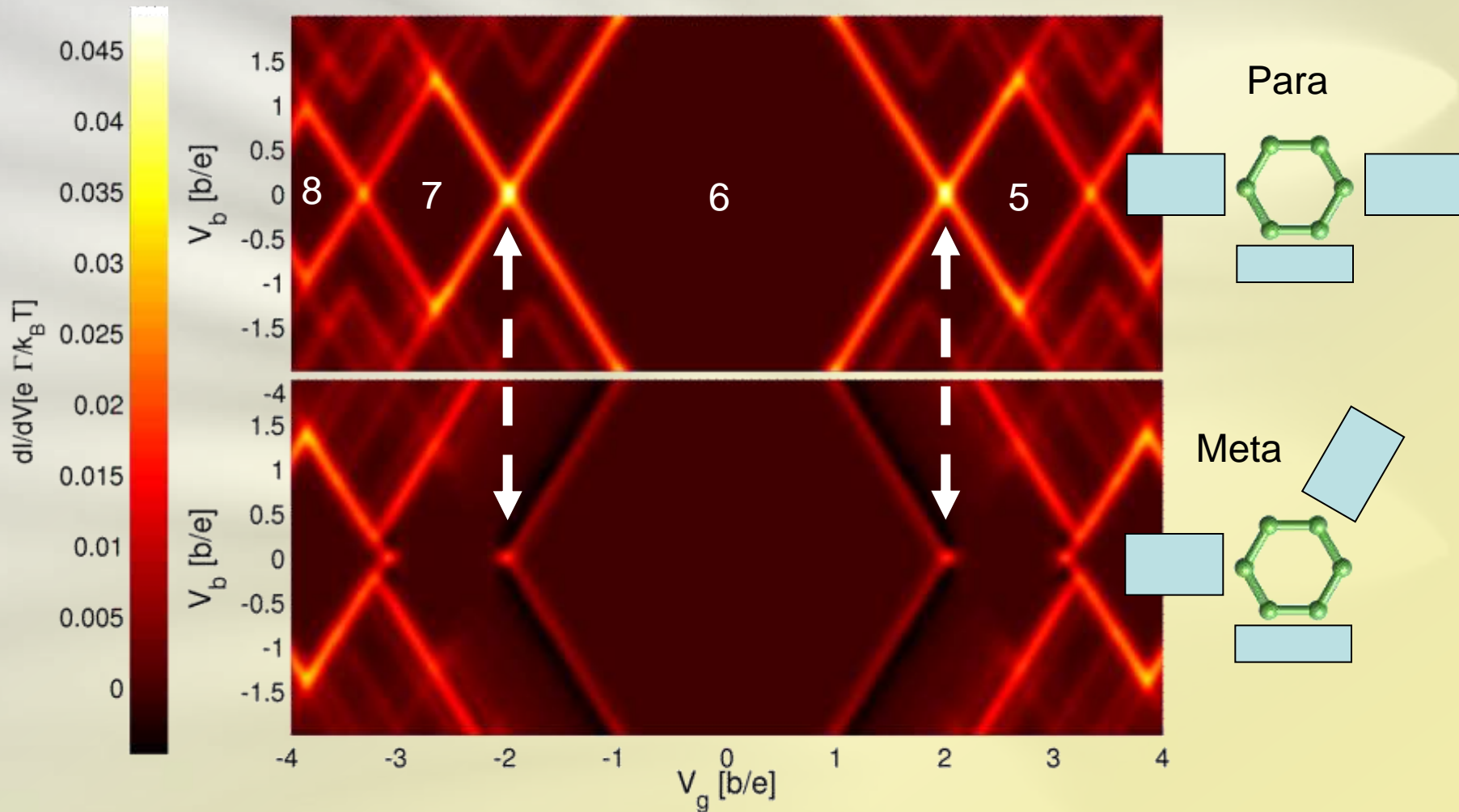
$$\Gamma_{ij}^X(E_1 - E_0) = \frac{2\pi}{\hbar} \sum_k (t_{ki}^X)^* t_{kj}^X \delta(\epsilon_k^X - E_1 + E_0)$$

For **uncorrelated** and **non-degenerate systems** the many-body rate reduces to

$$R_{N E_0 \rightarrow N+1 E_1}^{X\tau} = \Gamma_{\text{orb}}^X(\epsilon_{\text{orb}}) f^+(\epsilon_{\text{orb}} - \mu_X)$$



Conductance suppression

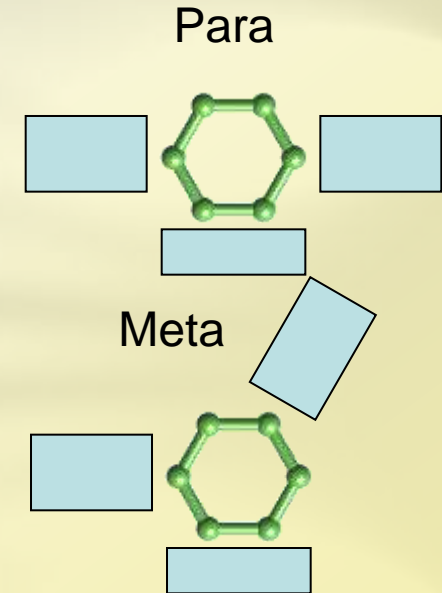
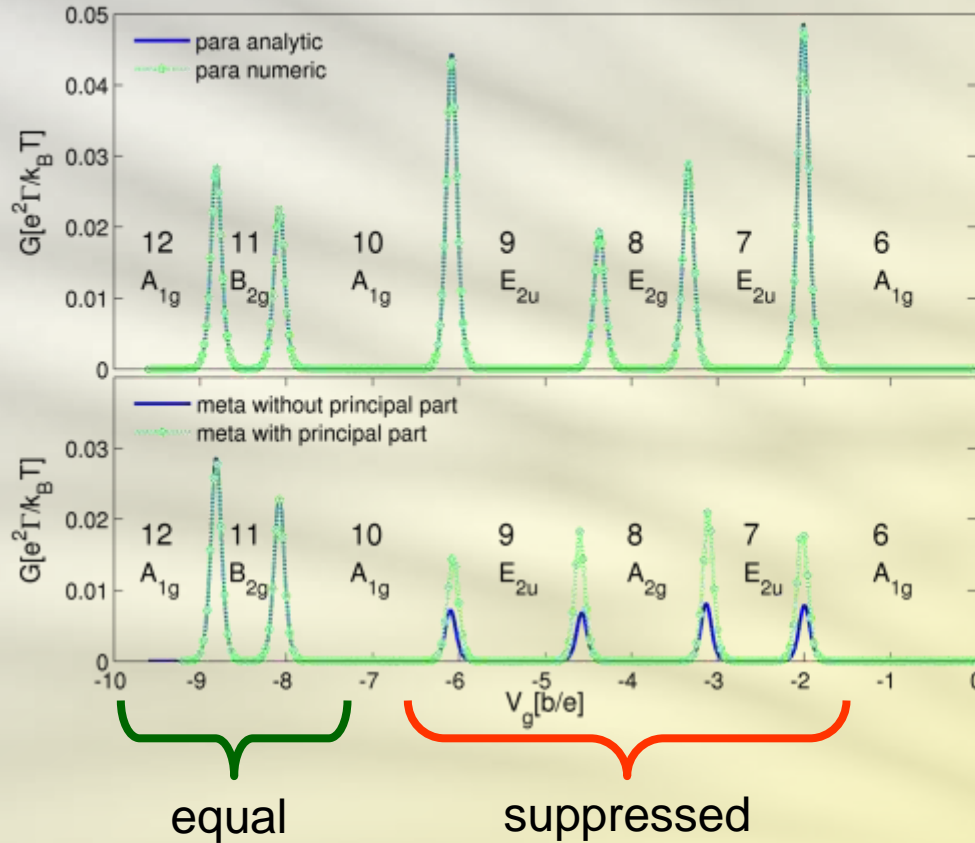


G. Begemann, D. Darau, **AD**, M. Grifoni, *Phys. Rev. B* **77**, 201406(R) (2008)

Regensburg - 10.02.2014

physikalisches

Conductance suppression



A: non-degenerate \longleftrightarrow **B:** non-degenerate \Rightarrow Equal

A: non-degenerate \longleftrightarrow **E:** degenerate \Rightarrow Suppressed

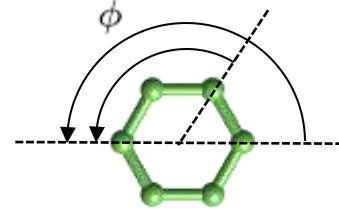
Destructive interference

$$\Lambda = \left| \sum_{nm\tau} \langle N, n | d_{L\tau} | N+1, m \rangle \langle N+1, m | d_{R\tau}^\dagger | N, n \rangle \right|^2$$

$$\Lambda = \left| \sum_{nm\tau} |\langle N, n | d_{L\tau} | N+1, m \rangle|^2 e^{i\phi_{nm}} \right|^2$$

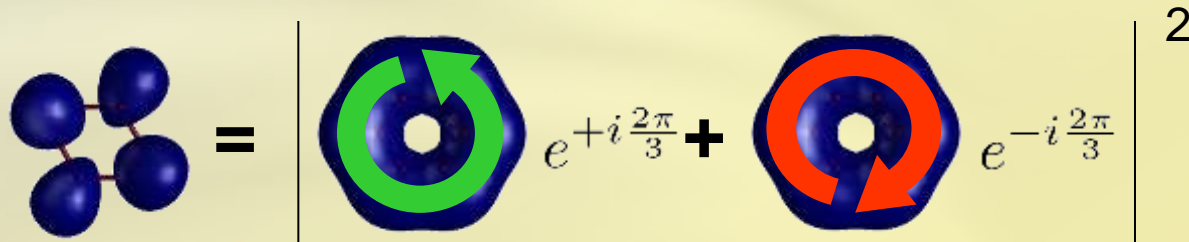
Interference factor

$$d_{R\tau}^\dagger = \mathcal{R}_\phi^\dagger d_{L\tau}^\dagger \mathcal{R}_\phi$$

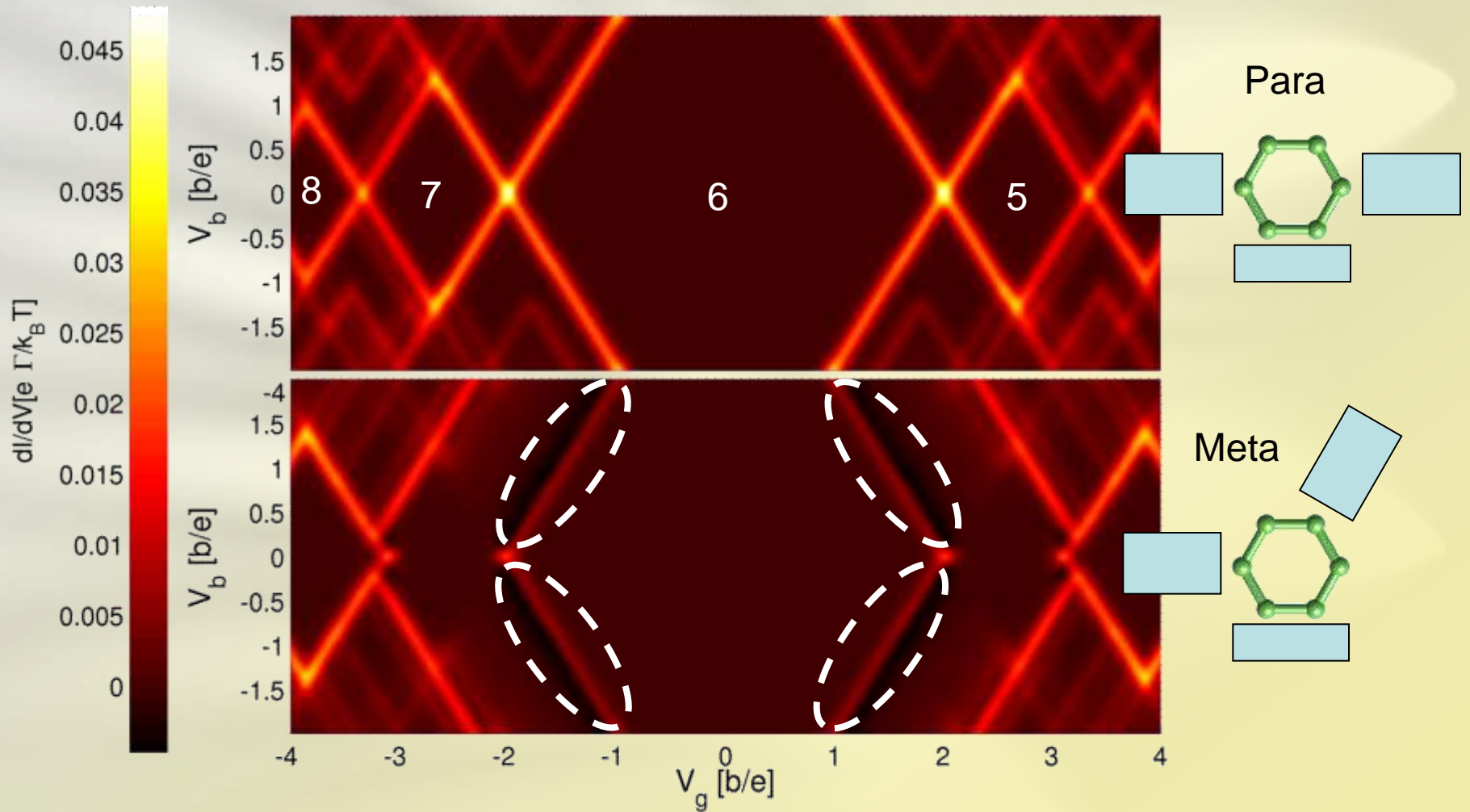


In particular for the transition **6-7** in the **meta** configuration:

$$\Lambda = \left| |\langle 6_g | d_{L\tau} | 7_g, +2, \tau \rangle|^2 e^{+i\frac{2\pi}{3}} + |\langle 6_g | d_{L\tau} | 7_g, -2, \tau \rangle|^2 e^{-i\frac{2\pi}{3}} \right|^2$$



Interference blockade



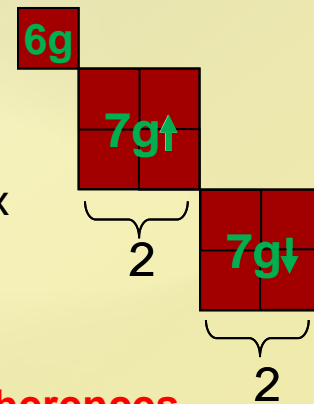
G. Begemann, D. Darau, **AD**, M. Grifoni, *Phys. Rev. B* **77**, 201406(R) (2008)

Regensburg - 10.02.2014

Visualization tool

$$P(x, y; \ell\tau) = \lim_{L \rightarrow \infty} \sum_{\sigma} \frac{1}{2L} \int_{-L/2}^{L/2} dz |\langle 7_g \ell\tau | \psi_{\sigma}^{\dagger}(\vec{r}) | 6_g \rangle|^2$$

- **Local transition probability** between states with **different** particle number, calculated in the physical basis
- **Physical basis**: the basis which diagonalizes the stationary density matrix
- The physical basis **depends on the bias**: in whatever reference basis, **coherences** are essential for a correct description of the system



Interference blockade

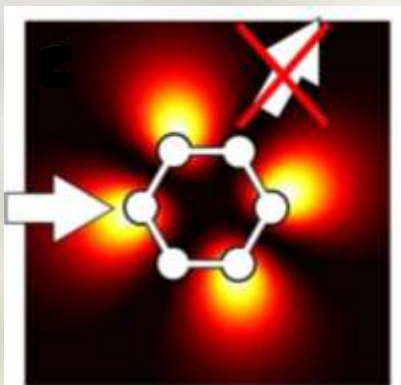


Geometry

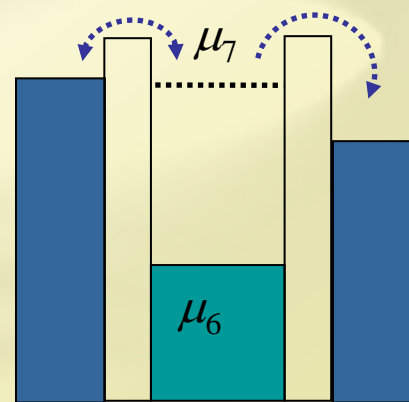
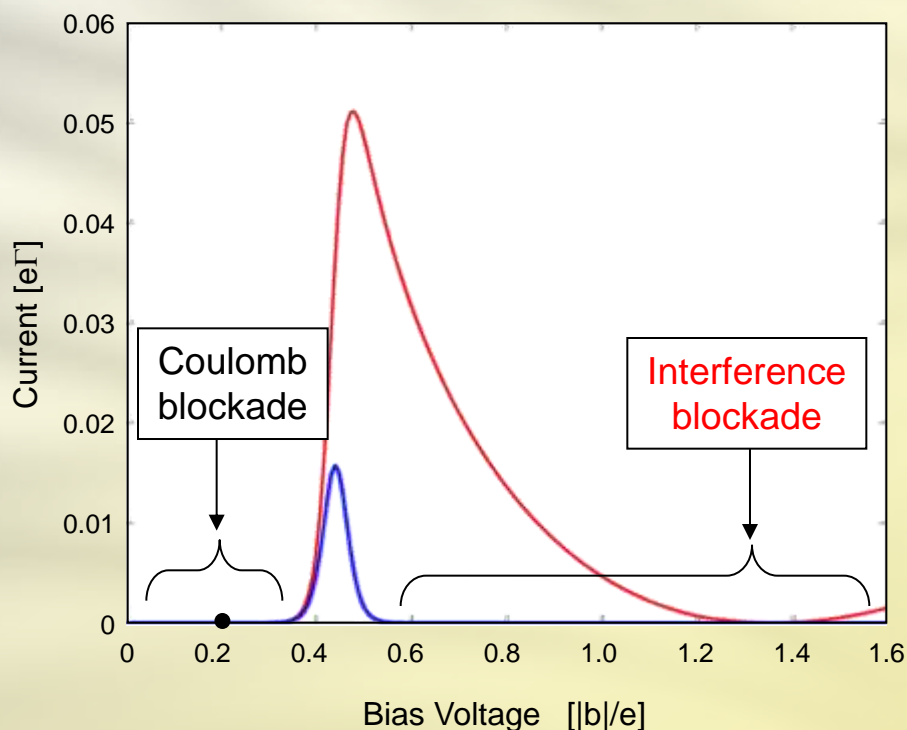
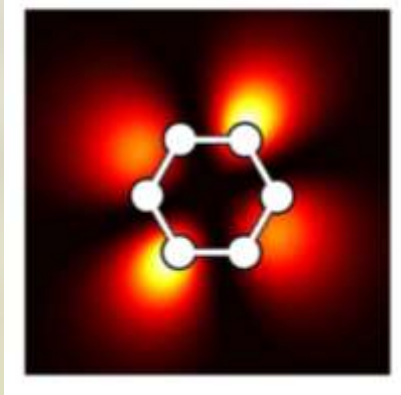
I-V for transition 6 -7

Energetics

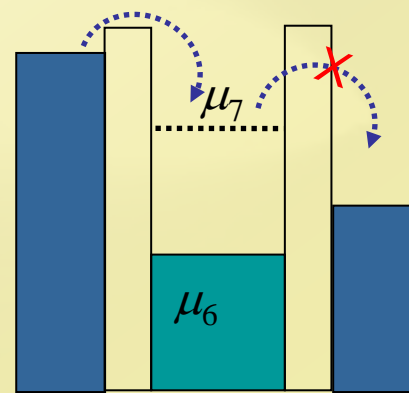
Blocking state



Non-blocking state



current onset

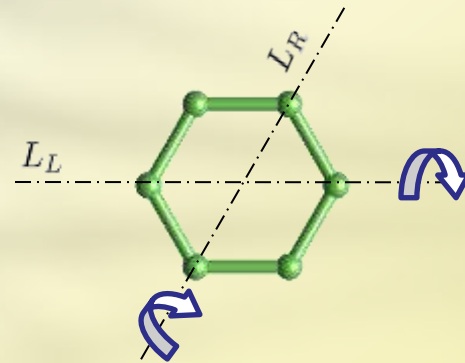


blockade

The effective Hamiltonian

The effective Hamiltonian is expressed in terms of **angular momentum** operators and **renormalization frequencies**:

$$H_{\text{eff}} = \sum_{\alpha\sigma} \omega_{\alpha\sigma} L_{\alpha}$$



In particular in the Hilbert space of the **7 particle ground states**

$$L_{\alpha} = \frac{\hbar}{2} \begin{pmatrix} 1 & e^{i2|\ell|\phi_{\alpha}} \\ e^{-i2|\ell|\phi_{\alpha}} & 1 \end{pmatrix}$$

$$\omega_{\alpha\sigma} = \frac{1}{\pi} \sum_{\sigma' \{E\}} \Gamma_{\alpha\sigma'}^0 \left[\langle 7_g \ell \sigma | d_{M\sigma'} | 8\{E\} \rangle \langle 8\{E\} | d_{M\sigma'}^{\dagger} | 7_g m \sigma \rangle p_{\alpha}(E - E_{7_g}) + \langle 7_g \ell \sigma | d_{M\sigma'}^{\dagger} | 6\{E\} \rangle \langle 6\{E\} | d_{M\sigma'} | 7_g m \sigma \rangle p_{\alpha}(E_{7_g} - E) \right]$$

← Bias and gate dependent

Interference blockade

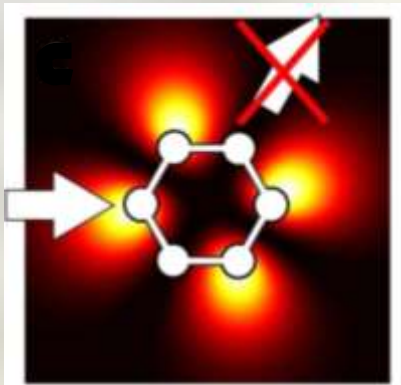


Geometry

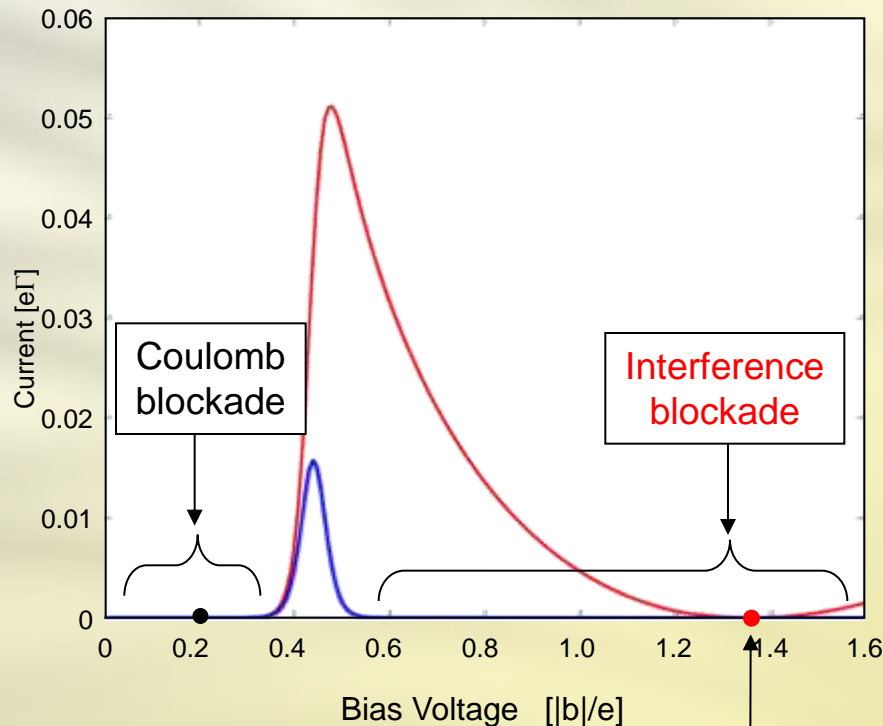
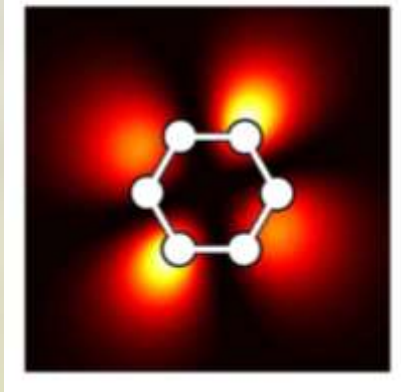
I-V for transition 6 -7

Energetics

Blocking state

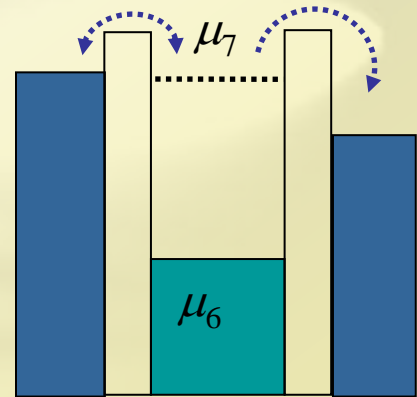


Non-blocking state

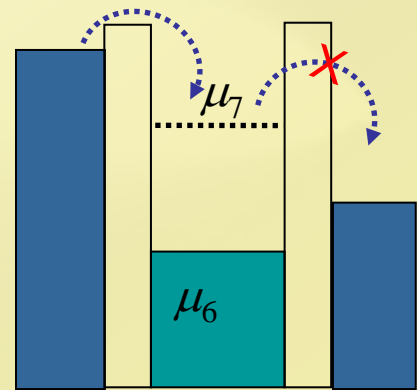


The **blocking** state is an eigenstate of the effective Hamiltonian

$$\omega_{L\sigma} = 0$$

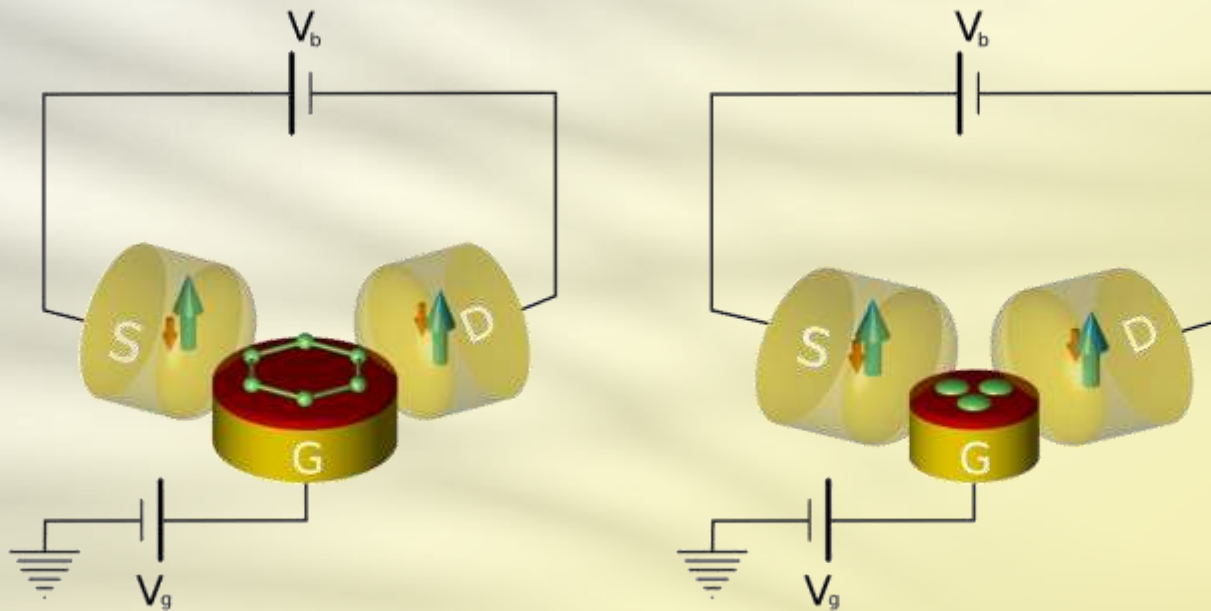


current onset



blockade

All-electrical spin control



AD, G. Begemann, and M. Grifoni *Nano Lett.* **9**, 2897 (2009)

AD, G. Begemann, and M. Grifoni *Phys. Rev. B*, **82**, 125451 (2010)

I-SET with a magnetic flavour

- **Coulomb** interaction
- Molecular **size**



Exchange splitting

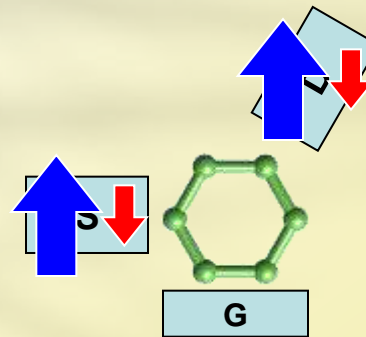


$$E_{\text{triplet}} \neq E_{\text{singlet}}$$

- Parallel **ferromagnetic** leads



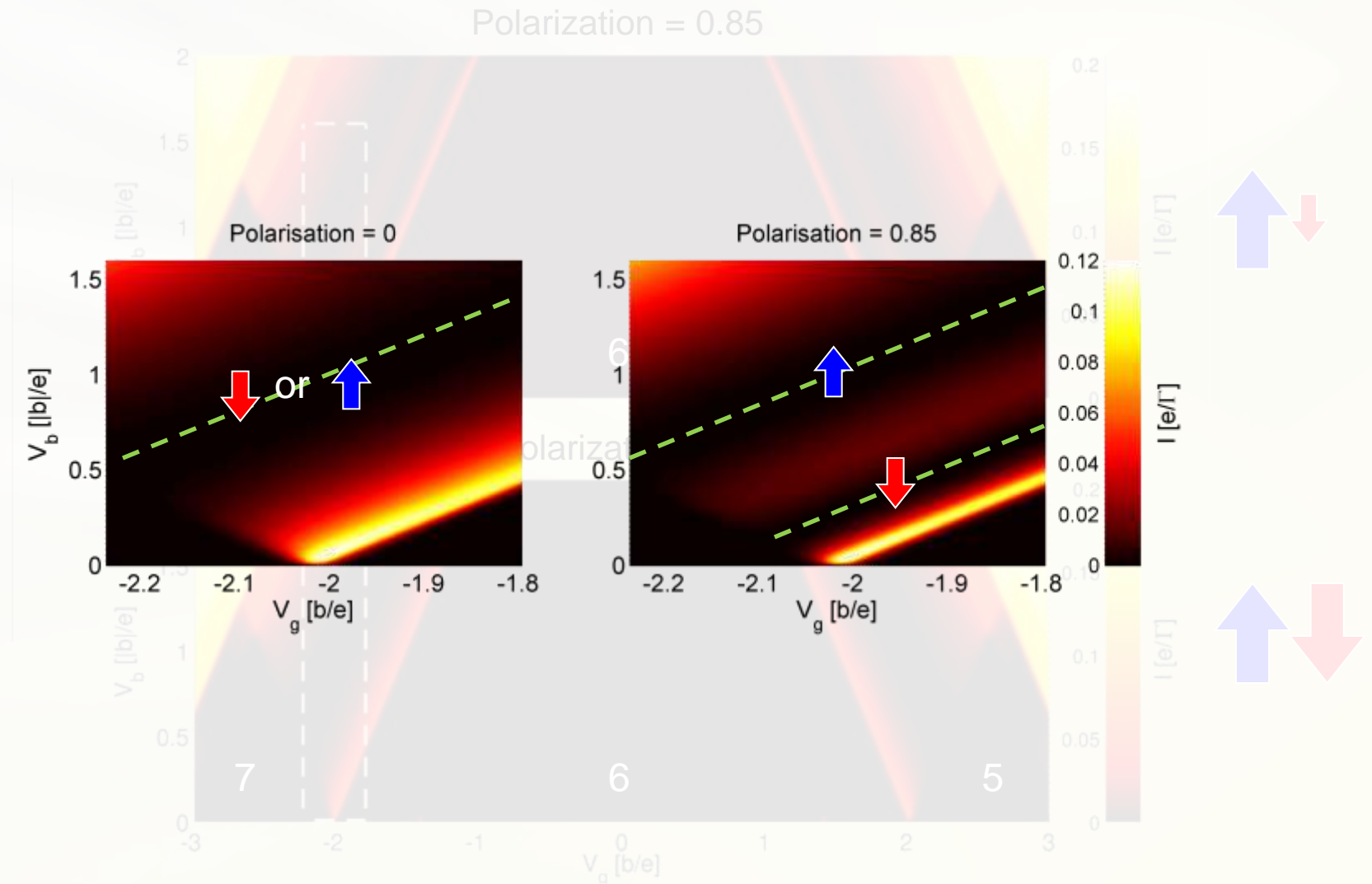
Spin symmetry breaking



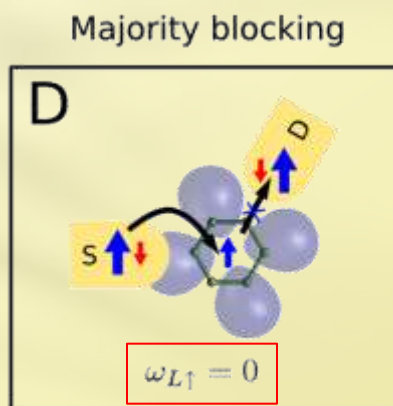
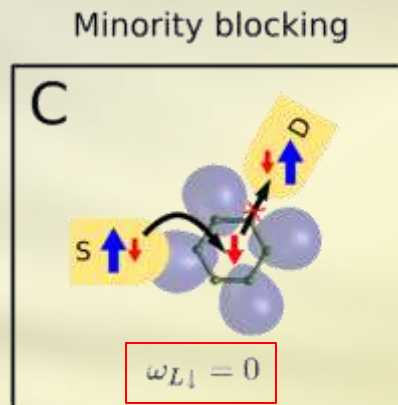
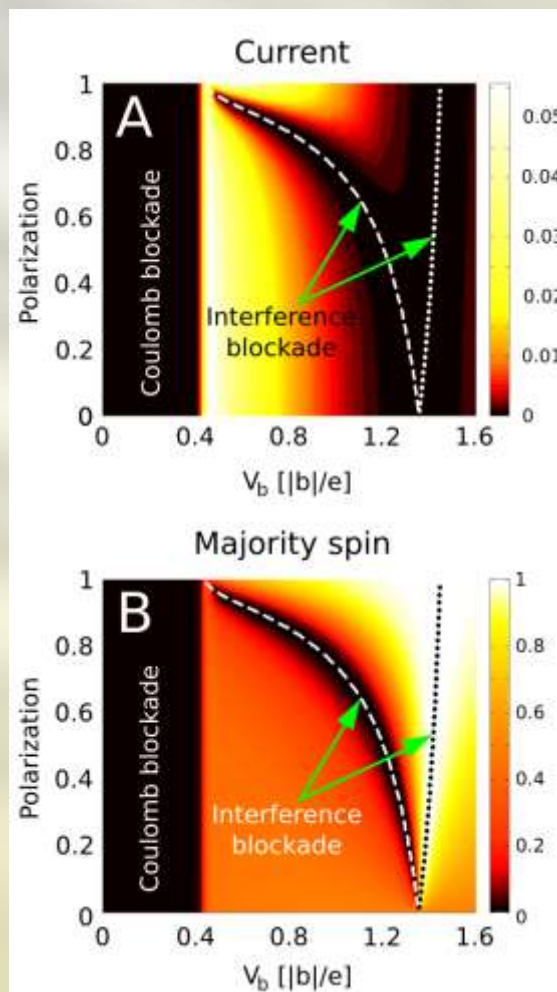
$$\Gamma_{\alpha\uparrow} \neq \Gamma_{\alpha\downarrow}$$

How do these properties translate into the **spin control** ?

Normal vs. ferromagnetic leads



Selective Interference Blocking



AD, G. Begemann, and M. Grifoni *Nano Lett.* **9**, 2897 (2009)

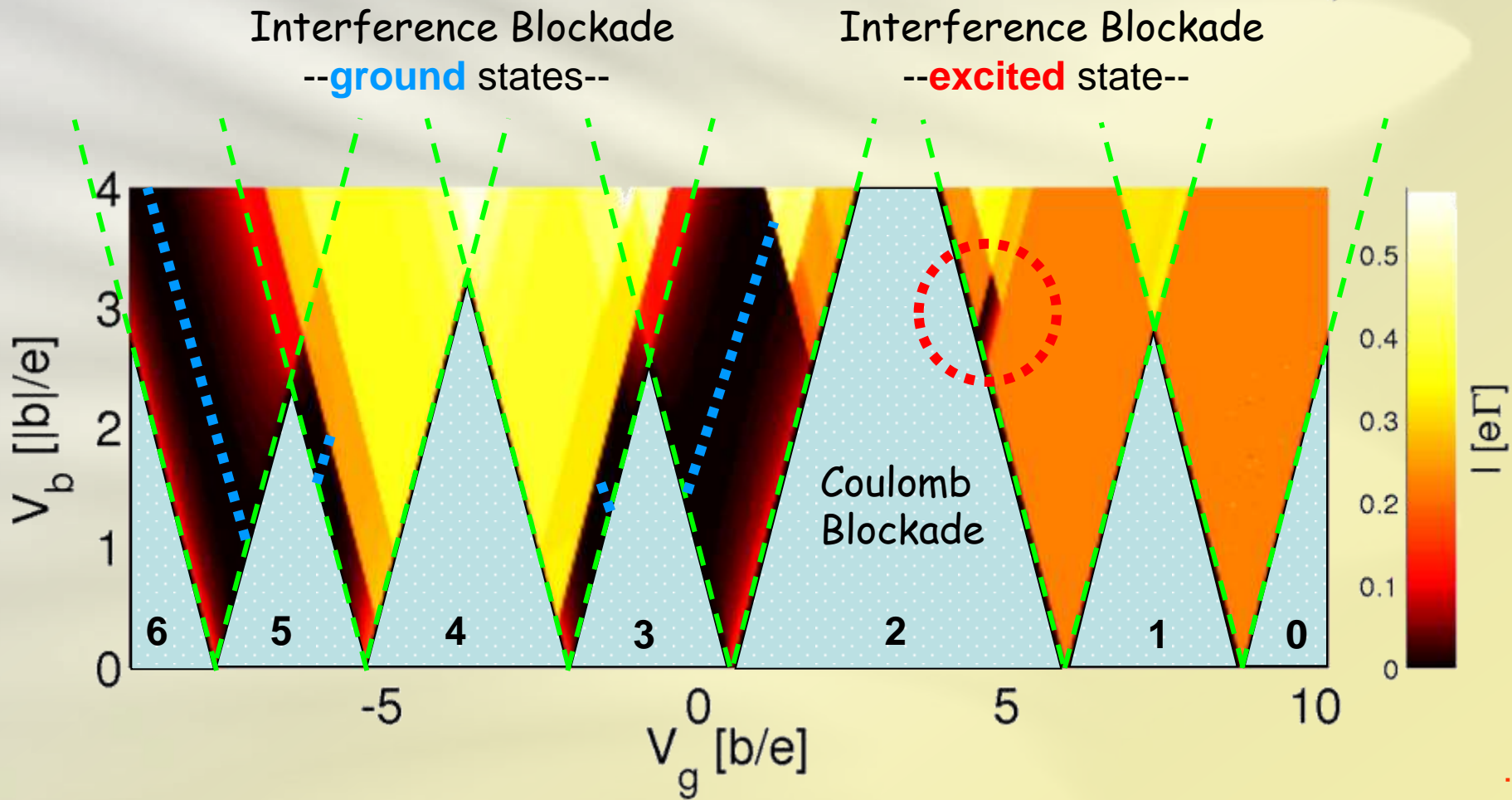
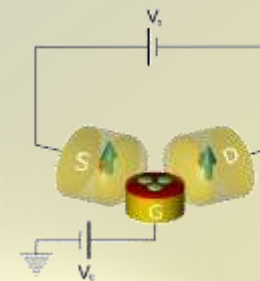
Level renormalization in presence of polarized leads

We obtain a difference in the renormalization frequencies for the 2 spin directions linear in the **polarization of the leads**:

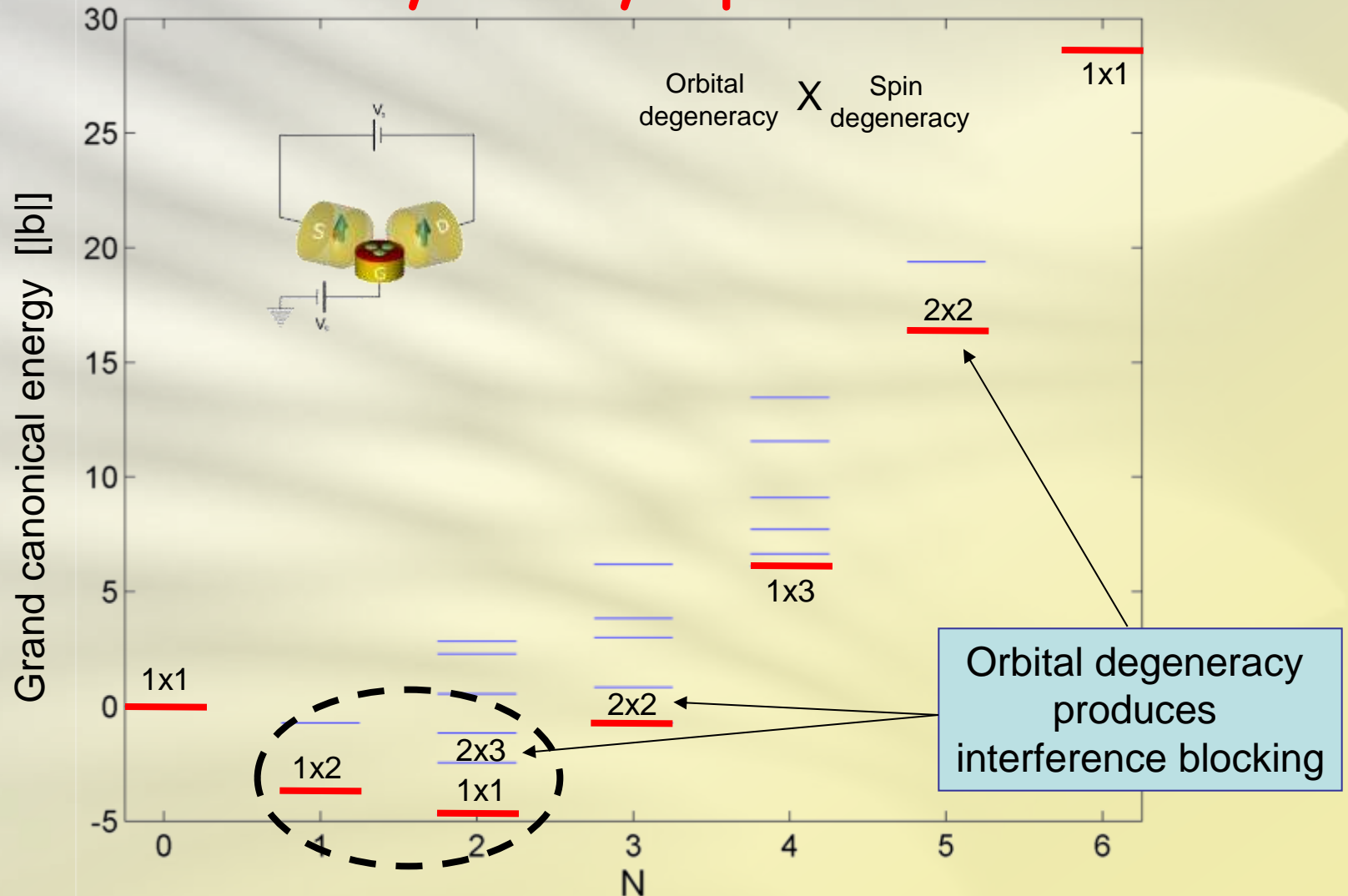
$$\omega_{\alpha\uparrow} - \omega_{\alpha\downarrow} = 2\bar{\Gamma}_{\alpha}^{-0} P_{\alpha} \frac{1}{\pi} \sum_{\{E\}} \left[\begin{aligned} &\langle 7_g \ell \uparrow | d_{M\uparrow} | 8\{E\} \rangle \langle 8\{E\} | d_{M\uparrow}^{\dagger} | 7_g m \uparrow \rangle p_{\alpha}(E - E_{7_g}) \\ &+ \langle 7_g \ell \uparrow | d_{M\uparrow}^{\dagger} | 6\{E\} \rangle \langle 6\{E\} | d_{M\uparrow} | 7_g m \uparrow \rangle p_{\alpha}(E_{7_g} - E) \\ &- \langle 7_g \ell \uparrow | d_{M\downarrow} | 8\{E\} \rangle \langle 8\{E\} | d_{M\downarrow}^{\dagger} | 7_g m \uparrow \rangle p_{\alpha}(E - E_{7_g}) \\ &- \langle 7_g \ell \uparrow | d_{M\downarrow}^{\dagger} | 6\{E\} \rangle \langle 6\{E\} | d_{M\downarrow} | 7_g m \uparrow \rangle p_{\alpha}(E_{7_g} - E) \end{aligned} \right]$$

The splitting of the level renormalization depends crucially on the Coulomb interaction on the molecule and **vanishes in absence of exchange**.

Triple dot ISET



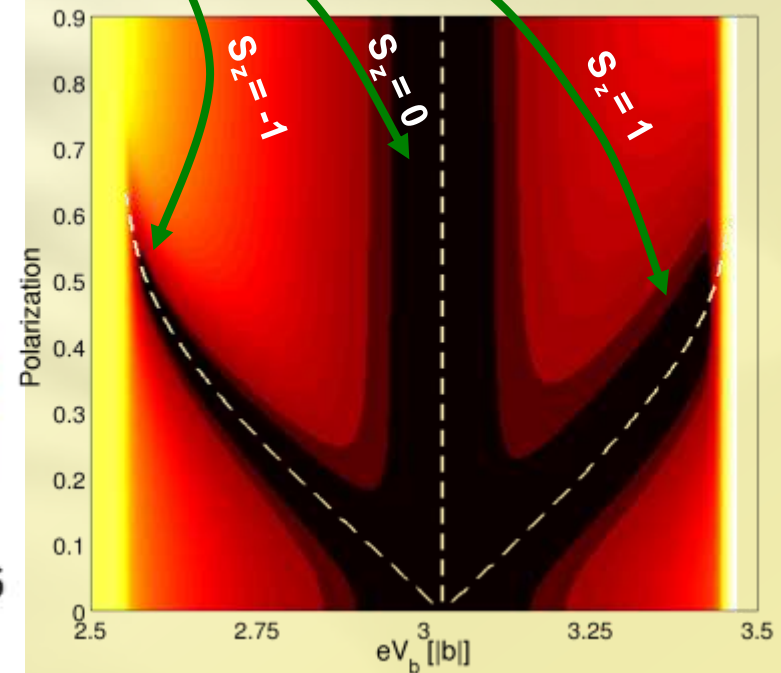
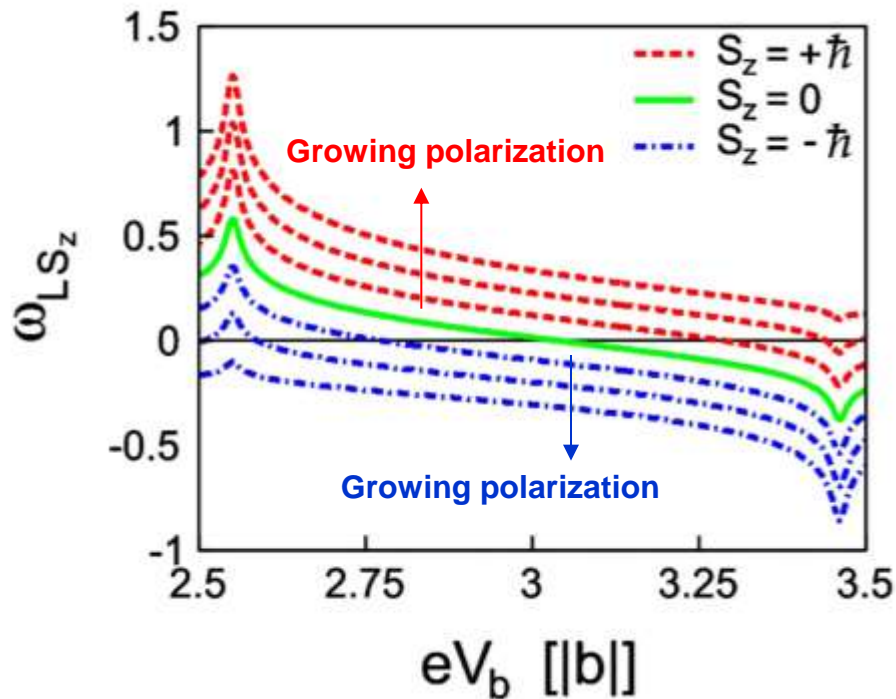
Many-body spectrum



Triplet splitting

The states decoupled from the right lead are eigenstates of L_R . They are eigenstates of H_{eff} only if

$$\omega_L S_z = 0$$

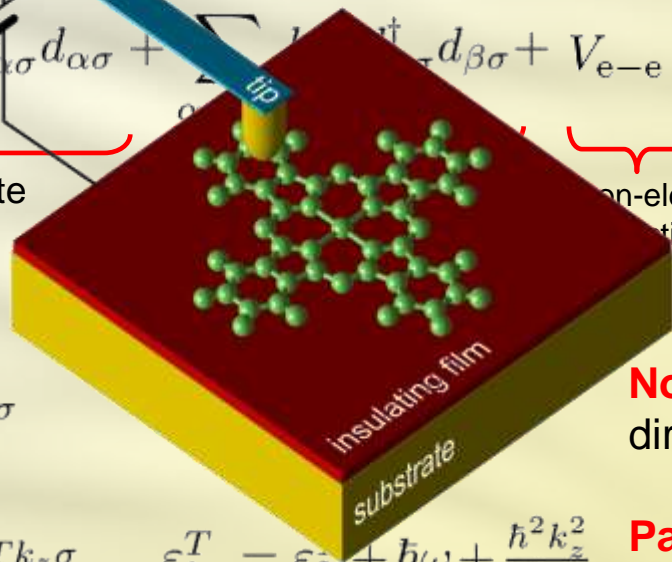


Topographical fingerprints

$$H = H_m + H_{\text{sub}} + H_{\text{tip}} + H_{\text{tun}}$$

$$H_m = \sum_{\alpha\sigma} \underbrace{V_{\alpha\alpha} d_{\alpha\sigma}^\dagger d_{\alpha\sigma}}_{\text{on-site}} + \sum_{\alpha\beta\sigma} \underbrace{t_{\alpha\beta} d_{\alpha\sigma}^\dagger d_{\beta\sigma}}_{\text{nearest-neighbor}} + \underbrace{V_{e-e}}_{\text{on-electron interaction}}$$

Hubbard
Extended Hubbard
Constant interaction



$$H_{\text{sub}} = \sum_{\vec{k}\sigma} \epsilon_{\vec{k}}^S c_{\vec{k}\sigma}^\dagger c_{\vec{k}\sigma}$$

No confinement in the x-y directions

$$H_{\text{tip}} = \sum_{k_z\sigma} \epsilon_{k_z}^T c_{T k_z\sigma}^\dagger c_{T k_z\sigma}$$

$$\epsilon_{k_z}^T = \epsilon_0 + \hbar\omega + \frac{\hbar^2 k_z^2}{2m}$$

Parabolic confinement in the x-y directions

$$H_{\text{tun}} = \sum_{\chi k i \sigma} t_{ki}^\chi c_{\chi k i \sigma}^\dagger d_{i\sigma} + h.c.$$

It is a **single particle** operator

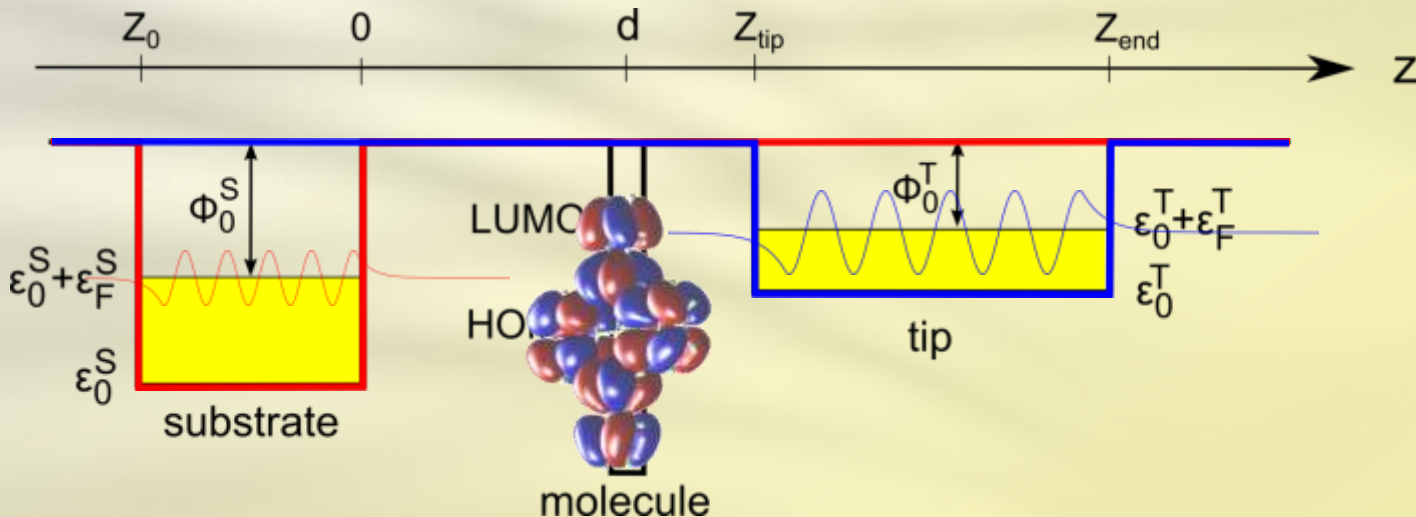
S. Sobczyk, AD, M. Grifoni, *Phys. Rev. B* **85**, 205408 (2012)

AD, B. Siegert, S. Sobczyk, M. Grifoni, *Phys. Rev. B* **86**, 155451 (2009)

Molecular orbital

Tunnelling amplitudes

$$h = \frac{p^2}{2m} + v_m + v_{\text{sub}} + v_{\text{tip}} \quad t_{ki}^\chi := \langle \chi k \sigma | h | i \sigma \rangle$$



S. Sobczyk, AD, M. Grifoni, *Phys. Rev. B* **85**, 205408 (2012)

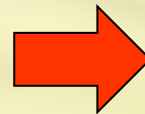
Tunnelling amplitudes (ii)

$$t_{ki}^{\chi} = \langle \chi k \sigma | \frac{p^2}{2m} + v_m | i \sigma \rangle + \langle \chi k \sigma | v_{\text{sub}} + v_{\text{tip}} | i \sigma \rangle$$

$$= \varepsilon_i \langle \chi k \sigma | i \sigma \rangle$$

Valence atomic orbitals
larger in the leads than
in the molecule

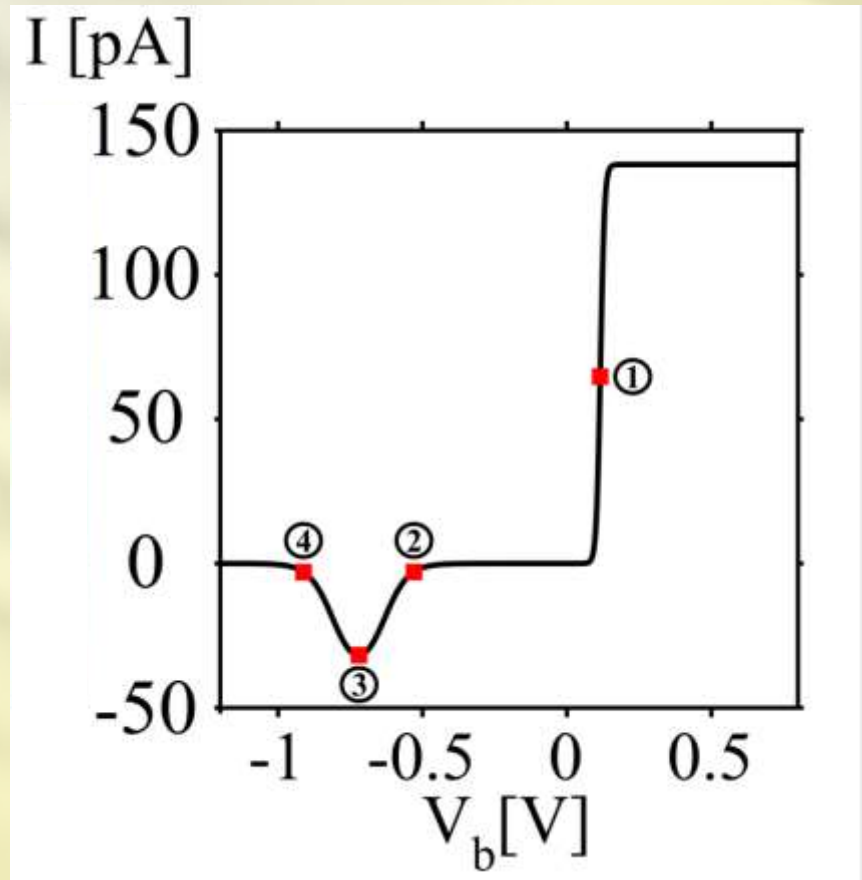
More perpendicular nodal planes
in the molecule than in the leads



$$\psi_{\chi k}(\vec{r}) \phi_i(\vec{r})$$

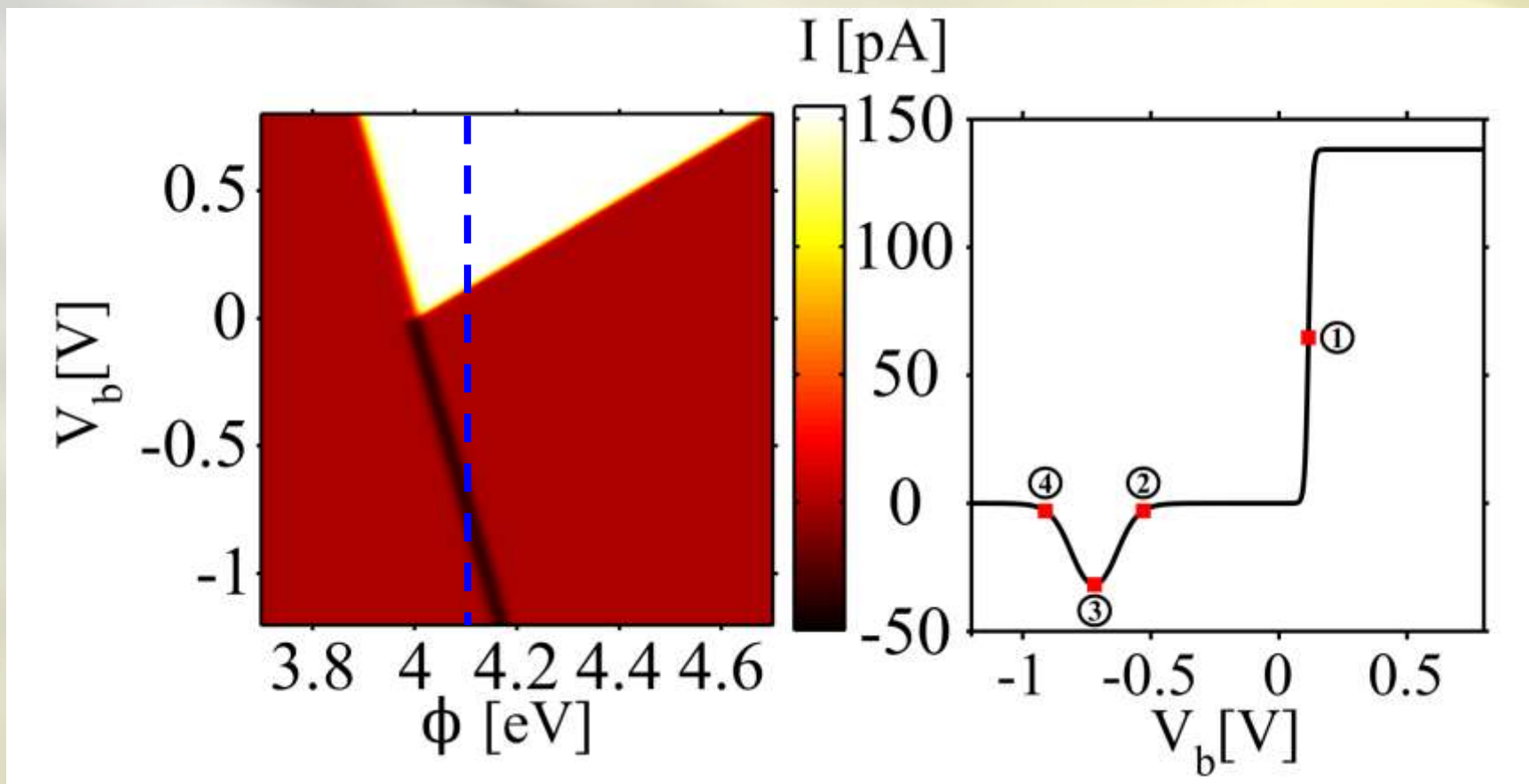
is **shifted towards
the molecule**

Interference blocking



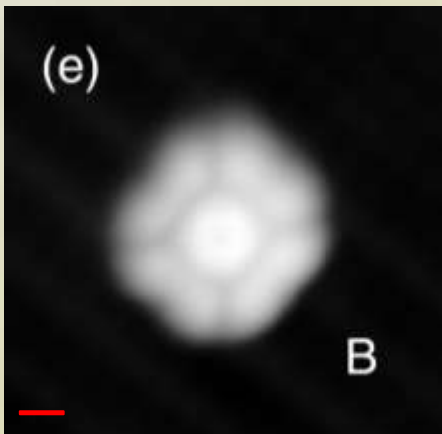
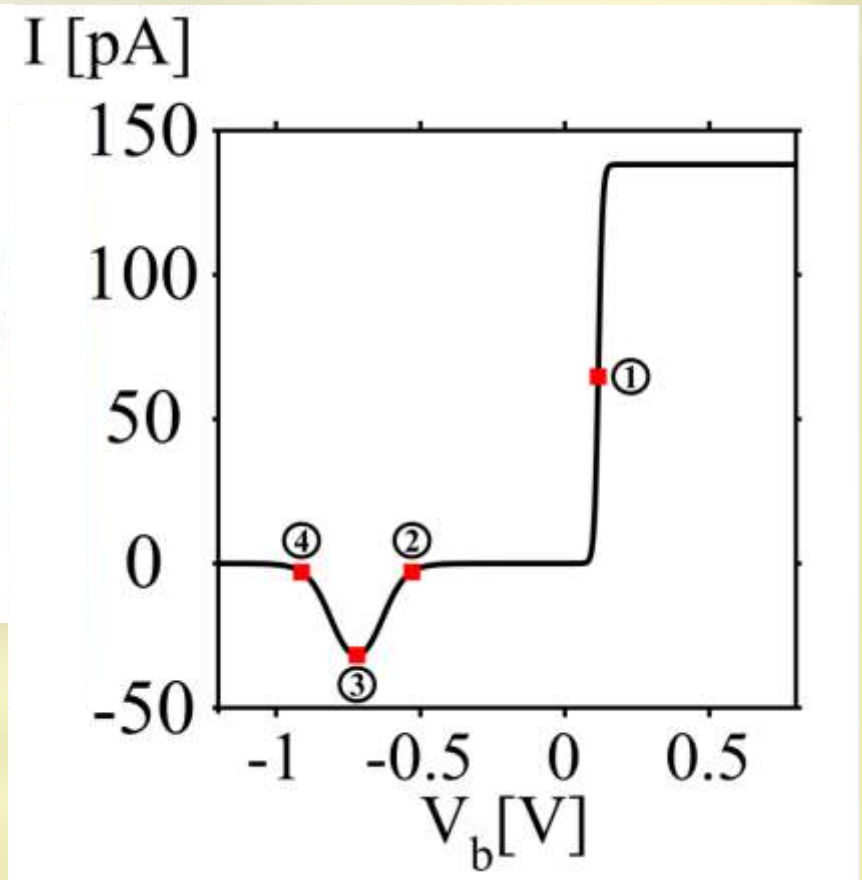
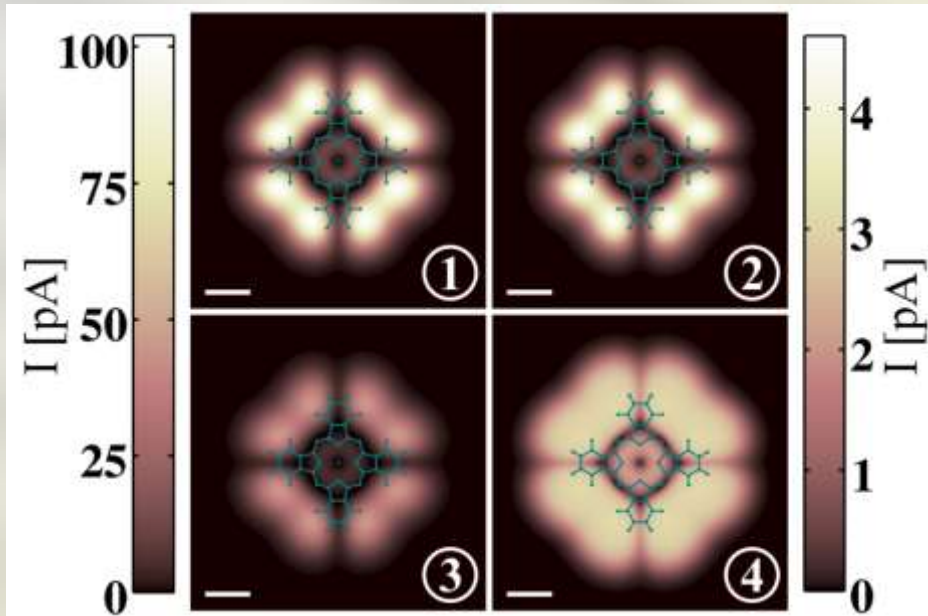
AD, B. Siegert, S. Sobczyk, M. Grifoni, *Phys. Rev. B* **86**, 155451 (2012)

Interference blocking



AD, B. Siegert, S. Sobczyk, M. Grifoni, *Phys. Rev. B* **86**, 155451 (2012)

Topographical fingerprint

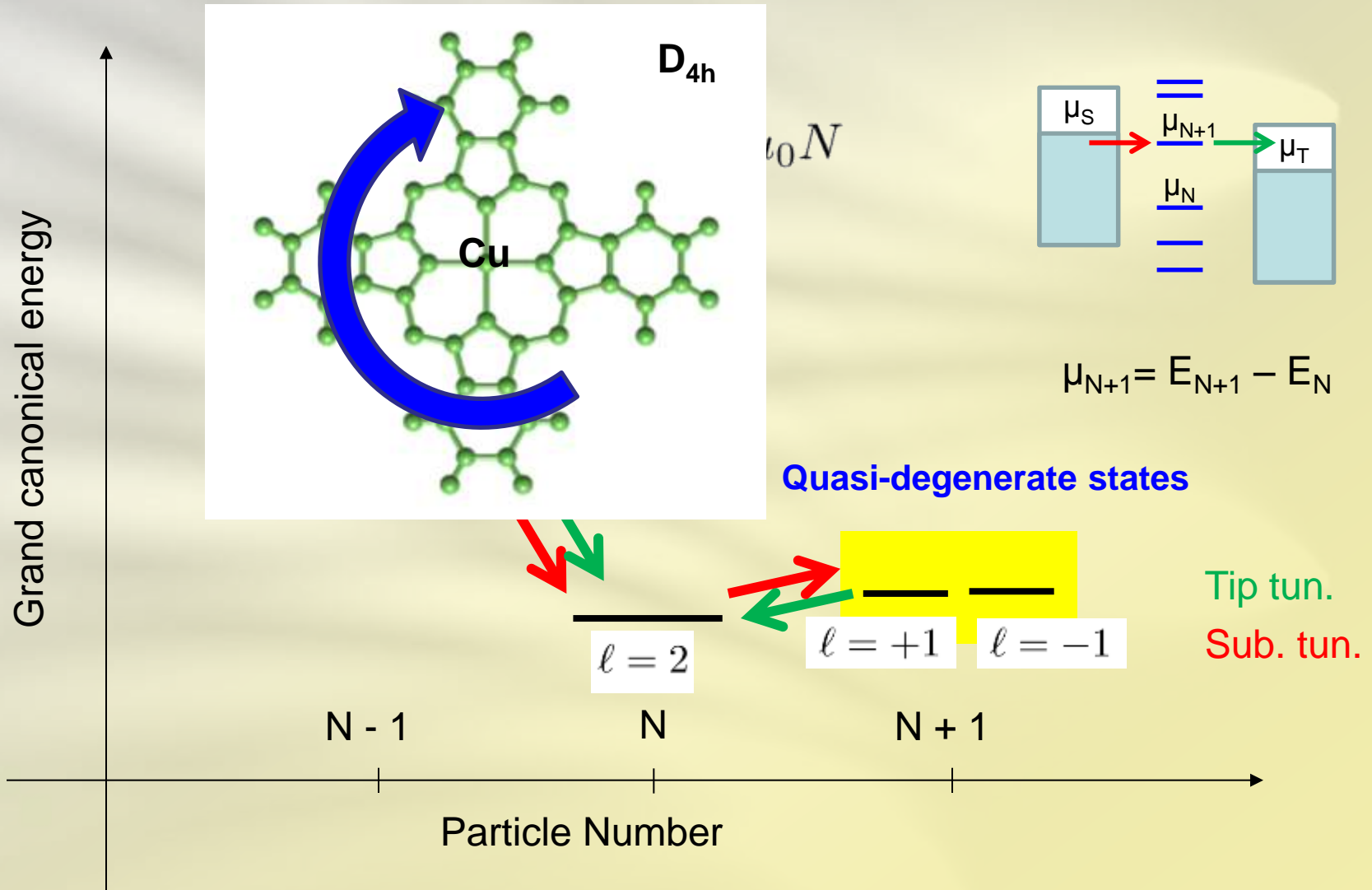


Experiment:
Cu-Pc on
two-atomic-layer NaBr

W. Ho et al.
PRL 100, 126807 (2008)

AD, B. Siegert, S. Sobczyk, M. Grifoni
Phys. Rev. B **86**, 155451 (2012)

Dynamics in energy space



Interference blocking in STM

Necessary conditions:

1. **Quasi-degeneracy** of the anionic ground state;
2. **Electron affinity** approximately **equals** the (effective) substrate **work function**.

Fingerprints:

1. **Strong negative differential conductance** at negative sample biases;
2. **Flattening** of the **constant height current images** in the vicinity of the interference blockade regime.

Interference: decoupling basis

Degenerate anionic ground state



Matrix form for the **many-body tunnelling rate** between the neutral and anionic ground states.

Angular momentum basis

Decoupling basis

Tip

$$\mathbf{R}^T = R_0^T \begin{pmatrix} \overset{\boxed{\ell = -1}}{1} & \overset{\boxed{\ell = -1}}{e^{-2i\phi}} \\ e^{-2i\phi} & 1 \end{pmatrix}$$

Mixes angular momentum

$$\tilde{\mathbf{R}}^T = R_0^T \begin{pmatrix} 2 & 0 \\ 0 & 0 \end{pmatrix}$$

One of the anionic state is **decoupled from the tip**

Substrate

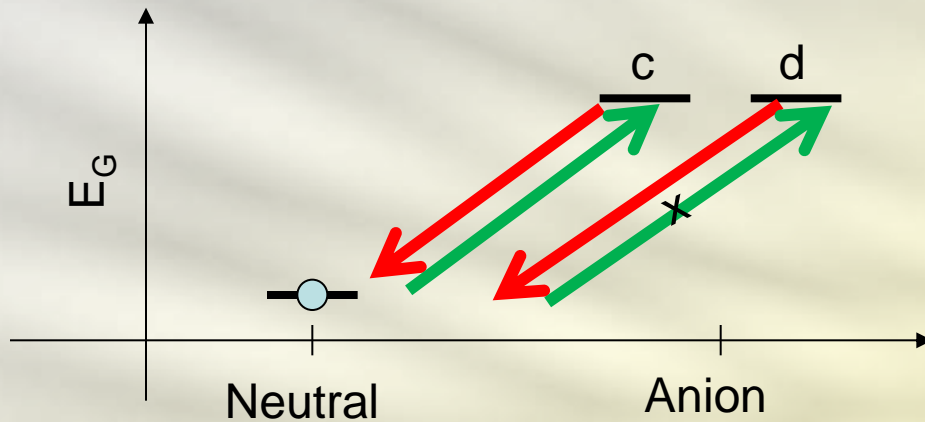
$$\mathbf{R}^S = R_0^S \begin{pmatrix} 1 & 0 \\ 0 & 1 \end{pmatrix}$$

Conserves angular momentum

$$\tilde{\mathbf{R}}^S = R_0^S \begin{pmatrix} 1 & 0 \\ 0 & 1 \end{pmatrix}$$

Notice that the decoupling basis **depends** on the **tip position**.

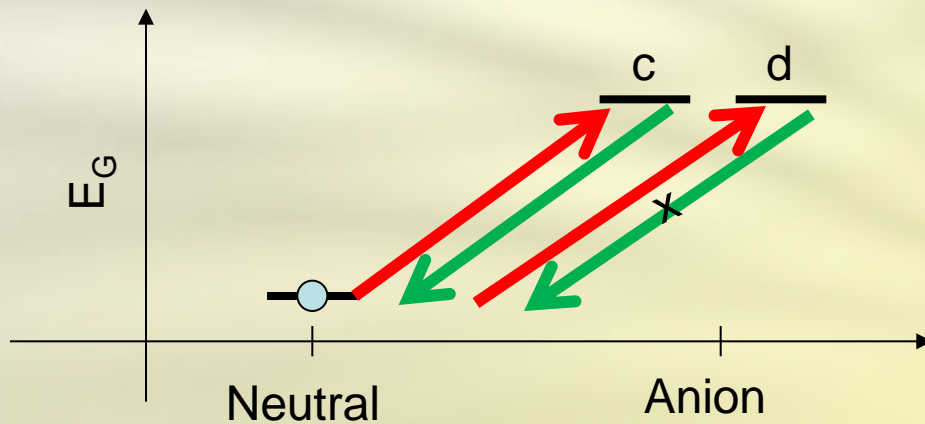
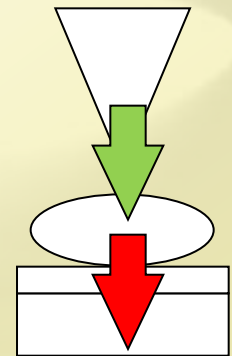
Interference: current blocking



$$V_b > -\Delta E_G / ec$$



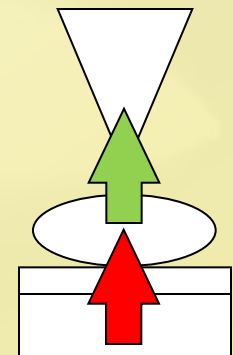
Current



$$V_b < \Delta E_G / e(1 - c)$$

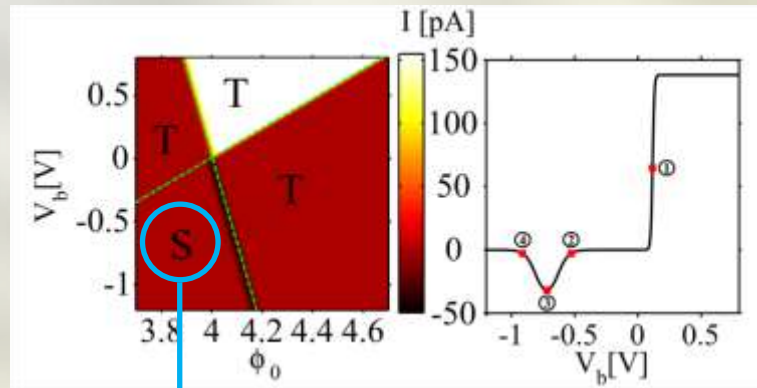


No current

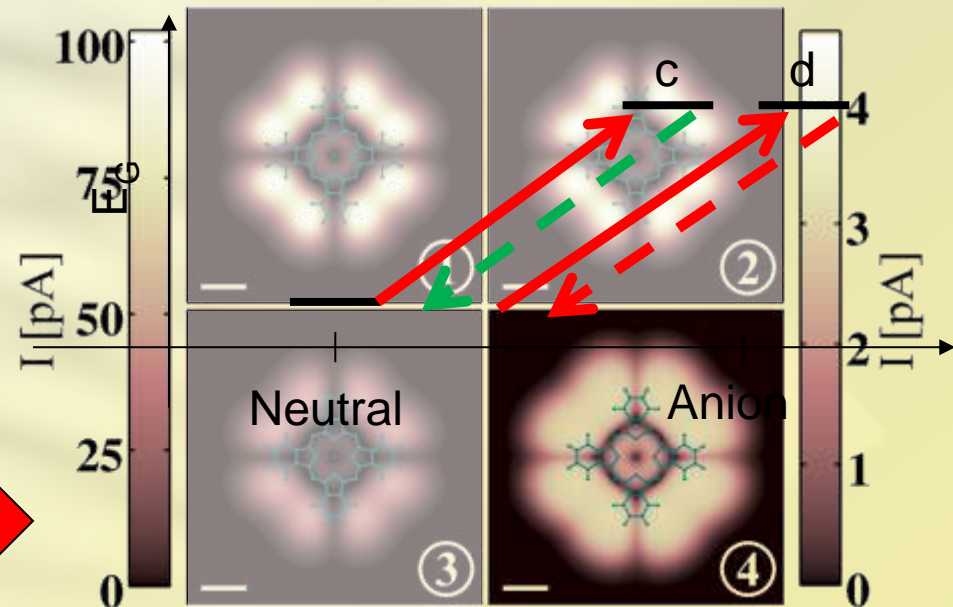
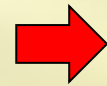


$$\mu_T = \mu_0 - ceV_b \quad \mu_S = \mu_0 + (1 - c)eV_b \quad c \approx 0.9$$

A new bottle-neck process

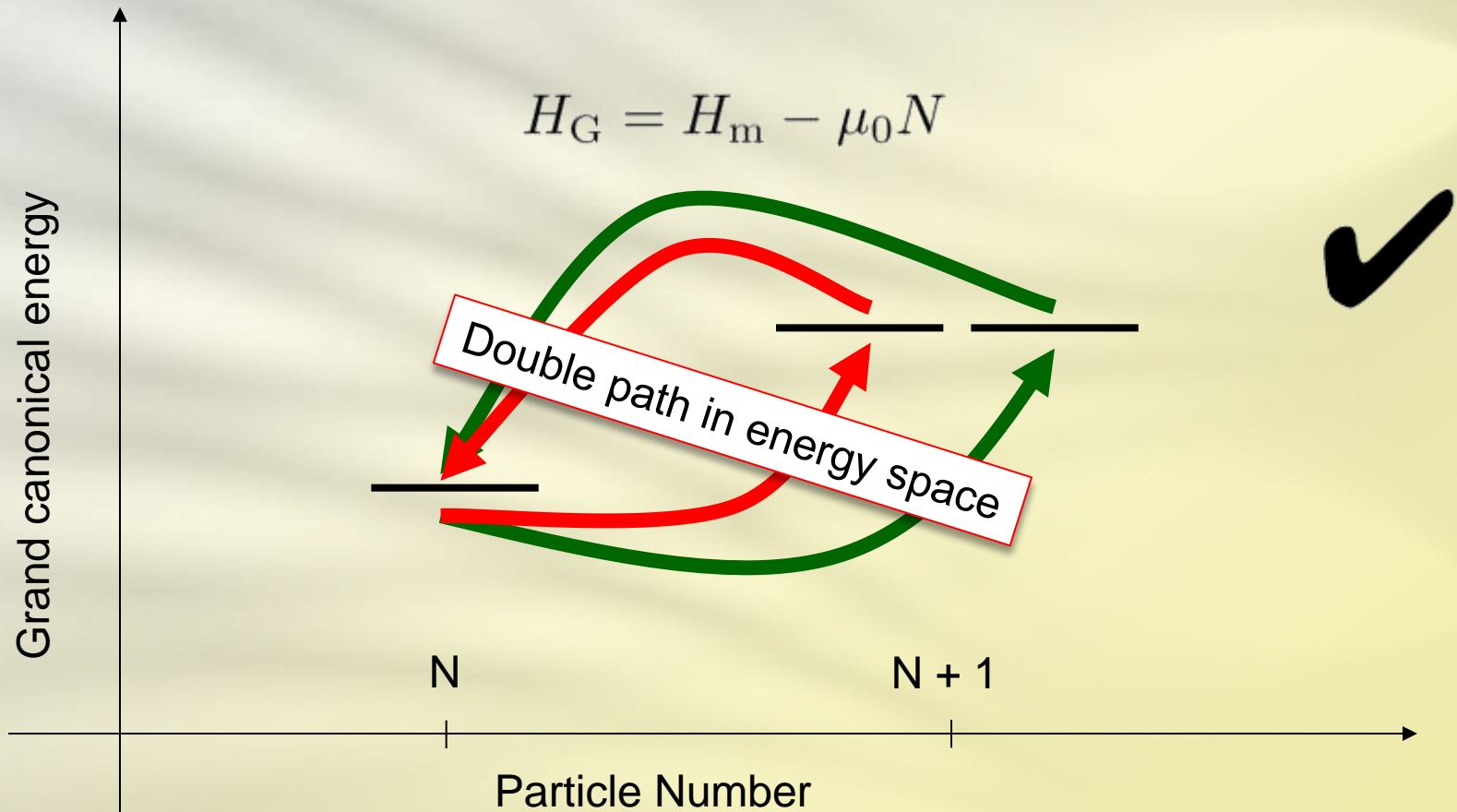


$$I_{IB} = e \frac{R_0^S f_S^- R_0^T f_T^-}{R_0^S f_S^- + R_0^T f_T^-}$$



The **depopulation** of the blocking state via a **substrate transition** dominates the transport.

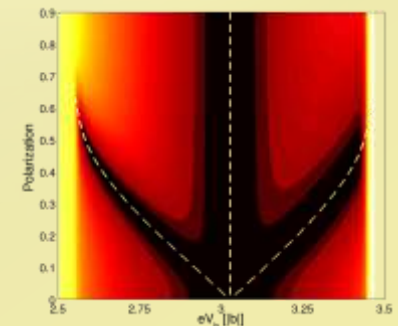
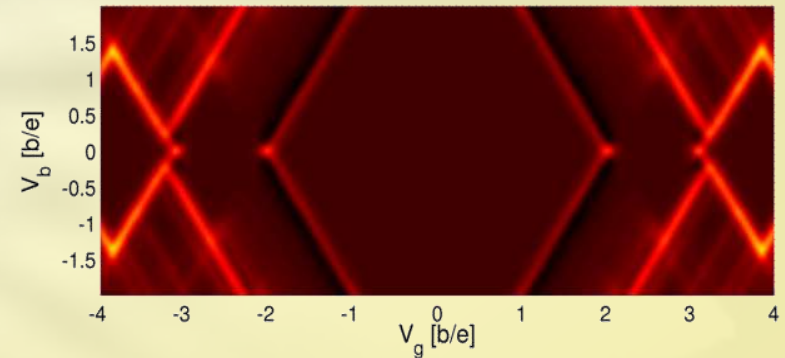
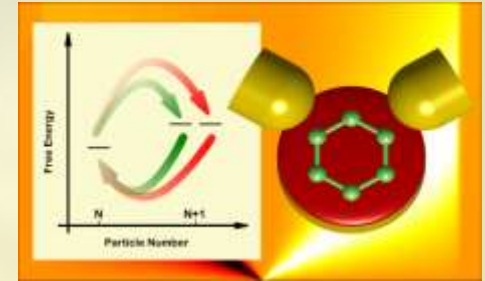
Interference + interaction



AD,G. Begemann, M. Grifoni, *Phys. Rev. B* **82**, 125451 (2010)

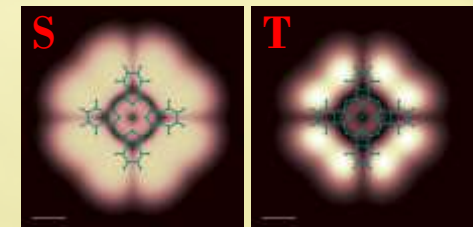
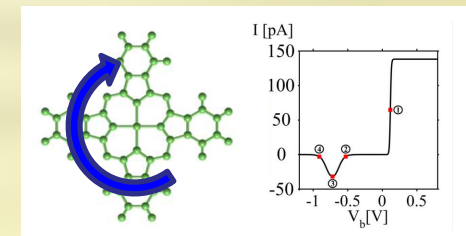
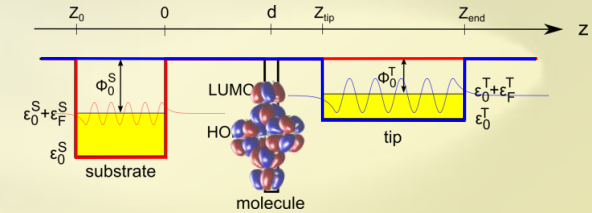
Conclusions

- Interference does occur even in the single-electron tunnelling regime when energetically equivalent paths involving **degenerate states** contribute to the dynamics.
- Interference effects dominates the transport characteristics of ISET both in the linear and non linear regime producing selective **suppression of the conductance** and interference **current blocking**.
- In the presence of ferromagnetic leads, the interplay between interference and exchange on the ISET allows to achieve **all-electrical spin control** of the junction.



Conclusions

- We developed a **semi-quantitative model** for the description of STM on thin insulating films
- Transport through **degenerate states** is associated to **electron interference** blockade at negative sample biases.
- Close to the interference blocking regime, substrate tunnelling dominates the transport and gives **flat constant height current maps**.



Interference Resonance

Outlook

- Include **molecular vibrations** to investigate their impact on interference phenomena
- Study the interplay between interference and molecular **spin anisotropy in** single molecule magnets
- Study the fingerprints of the interference blocking on the **current noise** or, more generally, on the full counting statistics of molecular junctions
- Include **higher order tunnelling** effects (co-tunnelling, Kondo)
- Investigate the relation between the **weak** and **strong coupling** interference effects
- Study the possibility of inducing or removing interference blocking via interaction with **light**

Thanks



Georg Begemann



Sandra Sobczyk



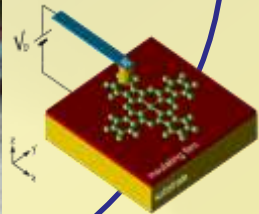
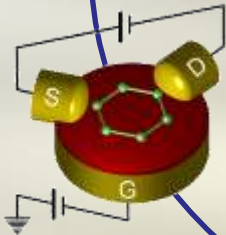
Milena Grifoni



Dana Darau



Benjamin Siegert



in the research programs

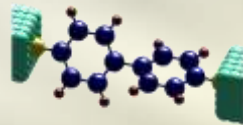


SFB 689 Spinphänomene
in reduzierten Dimensionen



SPP 1243 Quantum Transport
at the Molecular Scale

Vibronic effects and time-dependent transport through molecular nanojunctions

Phys. Rev. Lett. **97**, 166801 (2006)*Phys. Rev. B* **84**, 115432 (2011)*New J. Phys.* **14**, 023045 (2012)*Eur. Phys. J. B* **85**, 316 (2012)

A. Yar

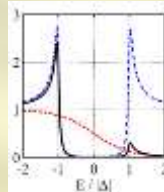


K. Richter



M. Grifoni

Transport through quantum dots with superconducting leads

Phys. Rev. B **87**, 155439 (2013)

S. Pfaller



S. Ratz



A. Hüttel



M. Grifoni



Ch. Strunk

Spin dependent transport through semiconducting quantum dots

Phys. Rev. B **77**, 245313 (2008)

R. Hornberger



S. Koller



M. Grifoni



S. Pfaller



S. Geißler

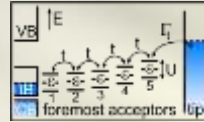


D. Weiss

Beside interference

XSTM on semiconductor surfaces

Phys. Rev. Lett. **111**, 216802 (2013)



G.Münnich



J.Repp



M.Wenderoth

Many-body localized molecular orbital approach to molecular transport

Phys. Rev. B **88**, 085404 (2013)



D.Ryndyk



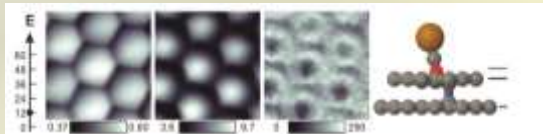
K.Richter



M.Grifoni



AFM and STM of graphene with a CO terminated tip



F.Gießibl



J.Waymouth



T.Hofmann

Spin-dependent transport through individual molecules



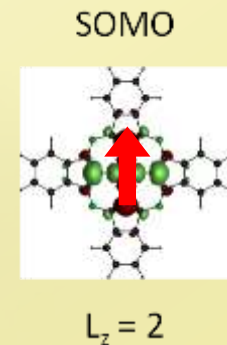
J.Repp



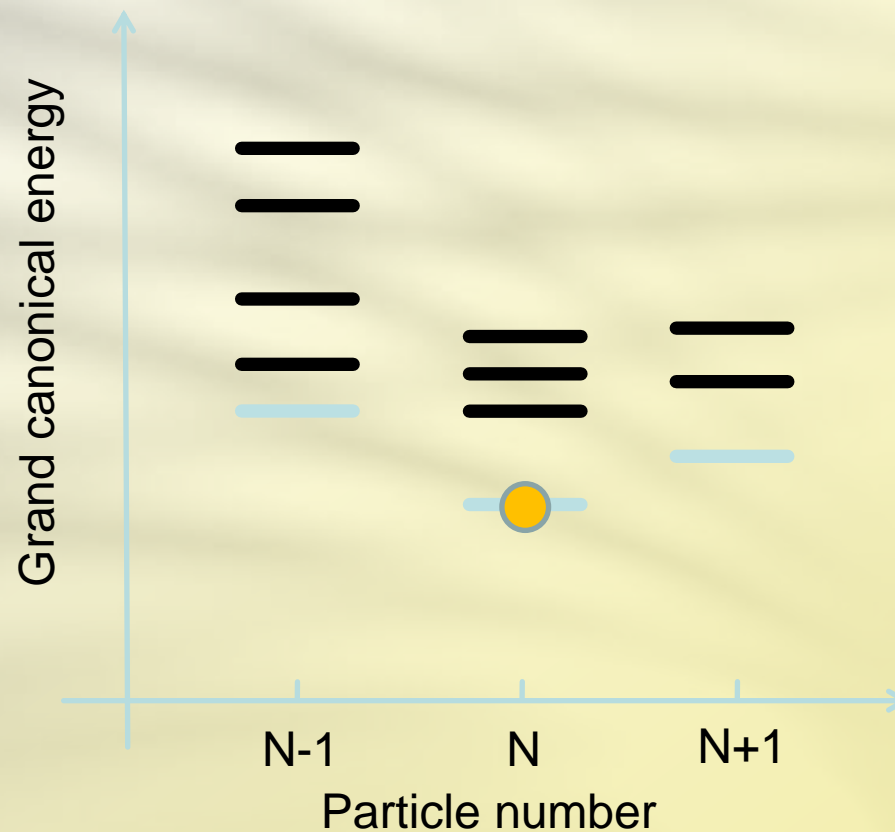
M.Grifoni



B.Siegert

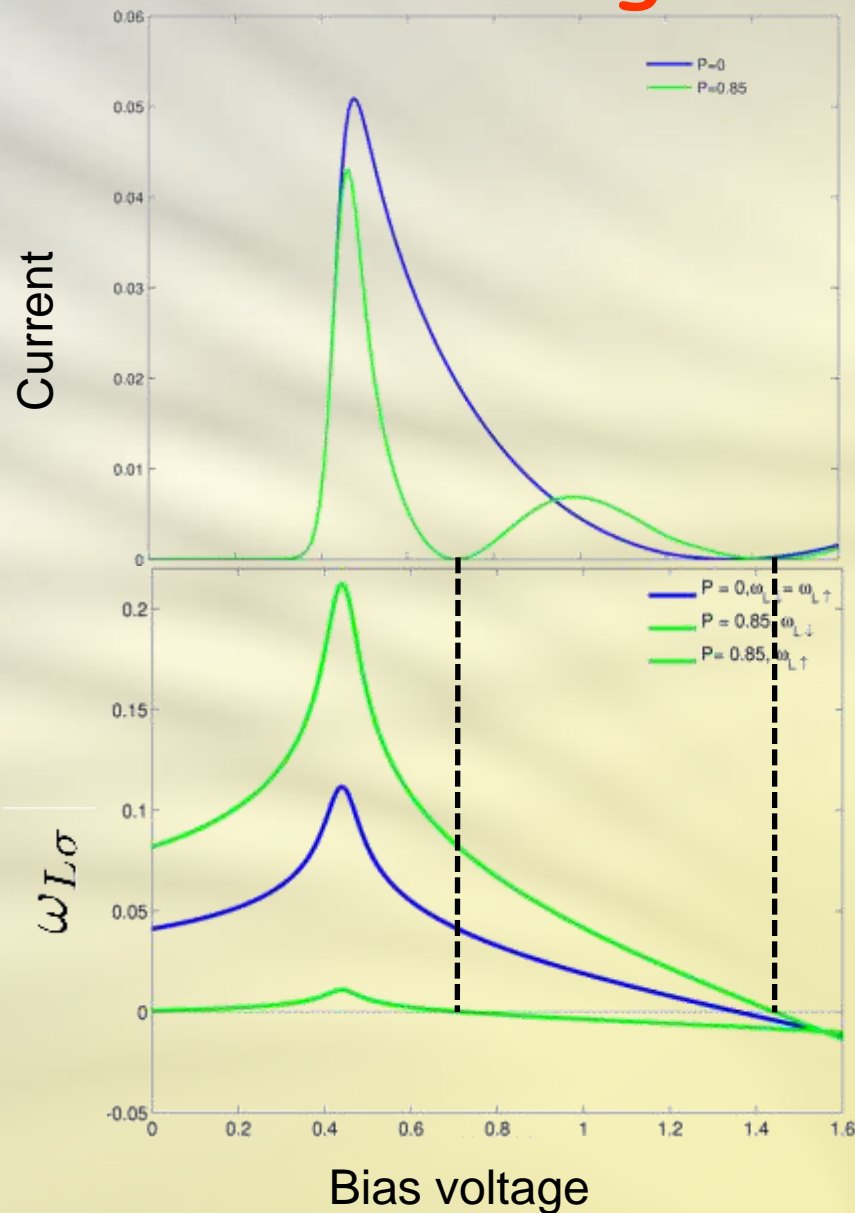


Thank you for your attention !

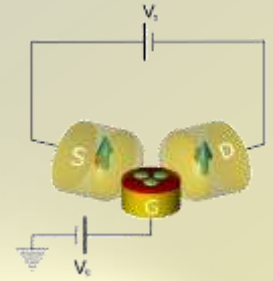


Supplementary material

Normal vs ferromagnetic leads



The triple dot ISET



$$H = H_{\text{sys}} + H_{\text{leads}} + H_{\text{tun}}$$

$$\begin{aligned}
 H_{\text{sys}} = & \xi_0 \sum_{i\sigma} d_{i\sigma}^\dagger d_{i\sigma} + b \sum_{i\sigma} \left(d_{i\sigma}^\dagger d_{i+1\sigma} + d_{i+1\sigma}^\dagger d_{i\sigma} \right) \\
 & + U \sum_i \left(n_{i\uparrow} - \frac{1}{2} \right) \left(n_{i\downarrow} - \frac{1}{2} \right) \\
 & + V \sum_i \left(n_{i\uparrow} + n_{i\downarrow} - 1 \right) \left(n_{i+1\uparrow} + n_{i+1\downarrow} - 1 \right)
 \end{aligned}$$

Extended Hubbard
Hamiltonian with on-site
and nearest neighbors
Coulomb interaction

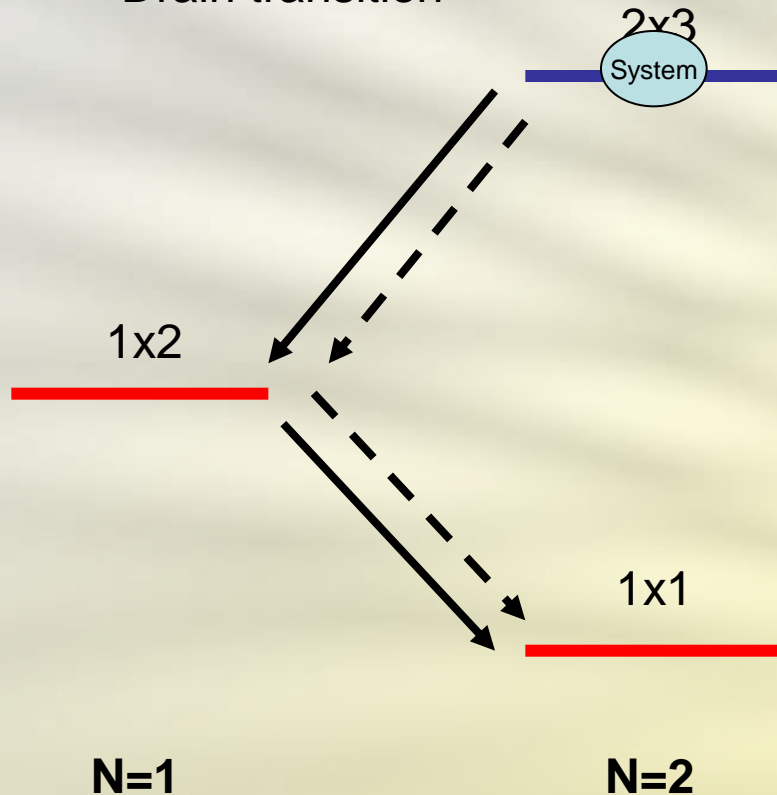
$$H_{\text{tun}} = t \sum_{\alpha k \sigma} \left(c_{\alpha k \sigma}^\dagger d_{\alpha \sigma} + d_{\alpha \sigma}^\dagger c_{\alpha k \sigma} \right)$$

← Tunnelling restricted to the dot
closest to the corresponding lead

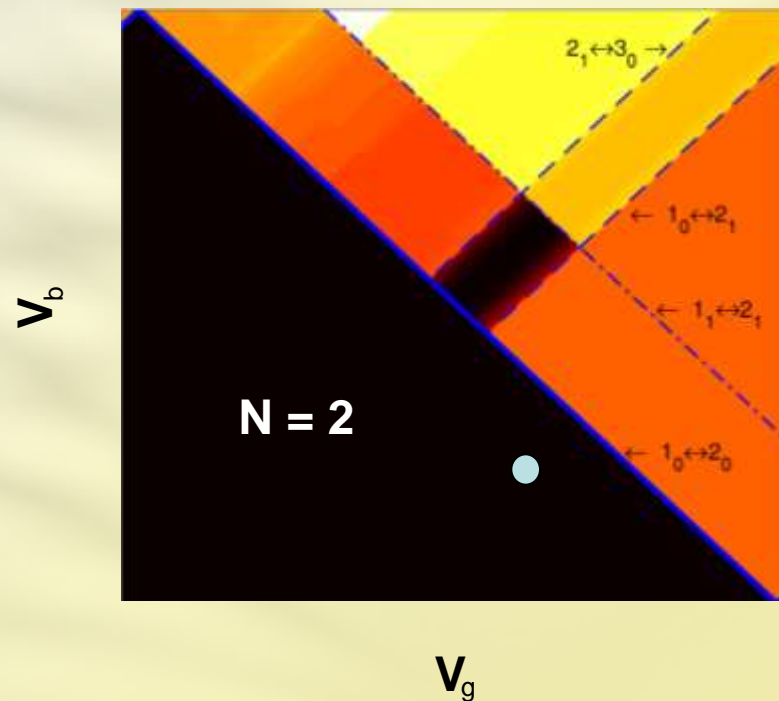
H_{leads} Ferromagnetic leads with equal parallel polarization

Excited state blocking

—▶ Source transition
 - -▶ Drain transition

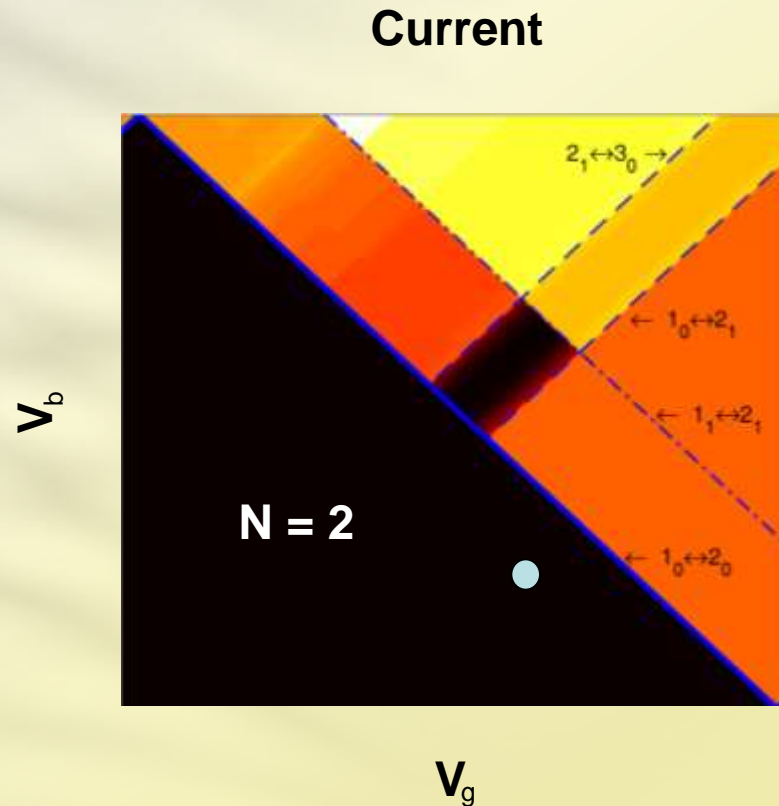
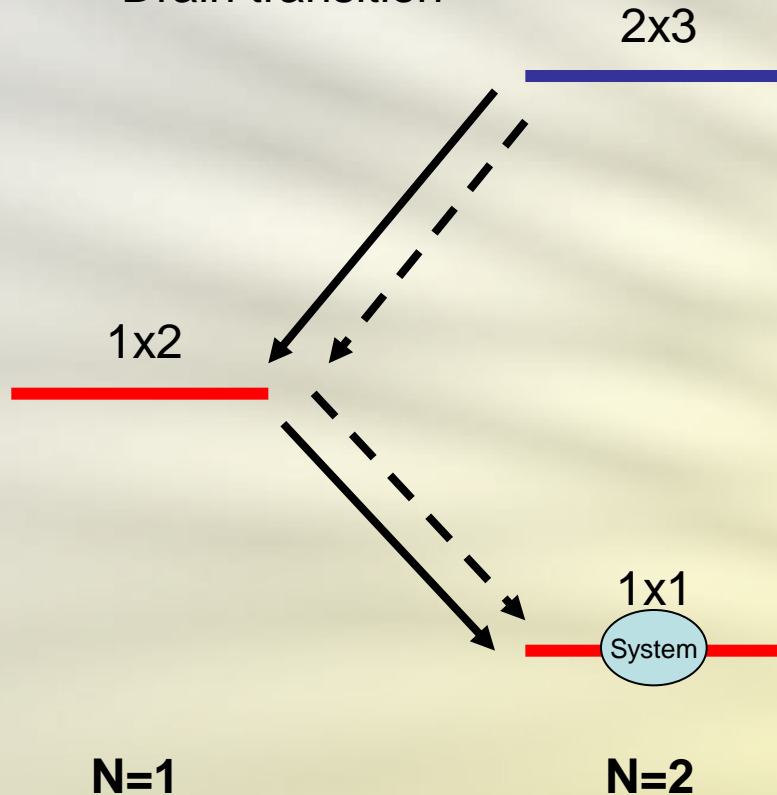


Coulomb Blockade



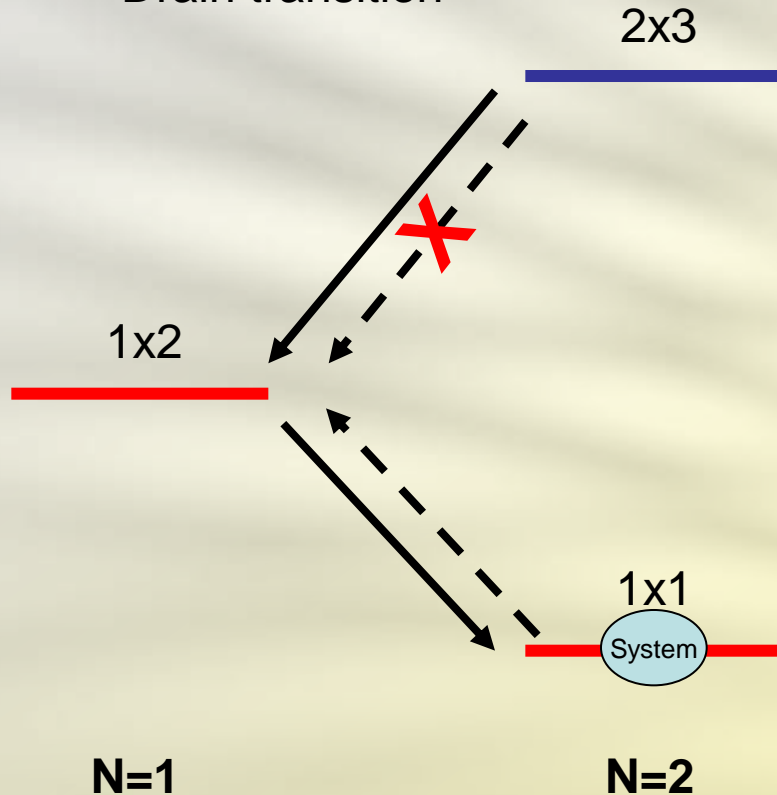
Excited state blocking

—▶ Source transition
 - -▶ Drain transition

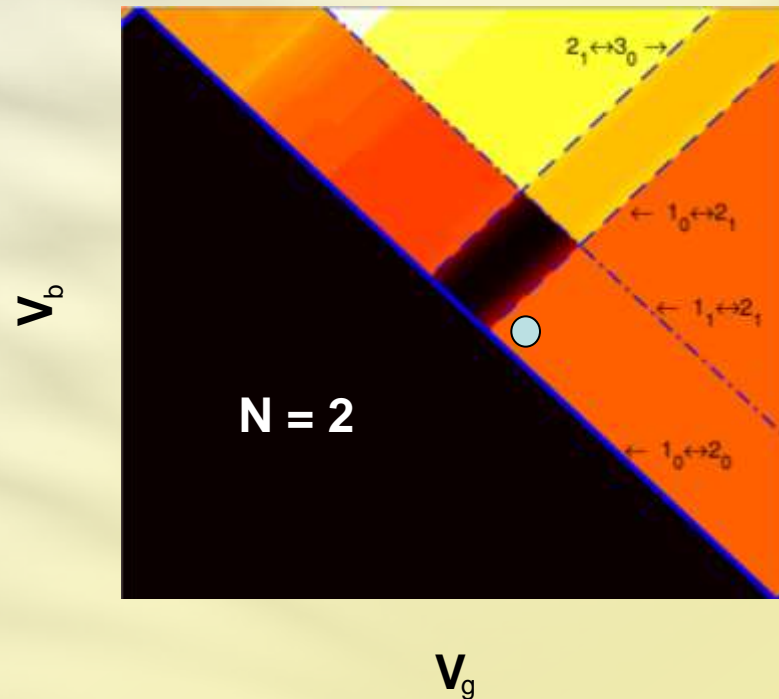


Excited state blocking

—▶ Source transition
 - -▶ Drain transition

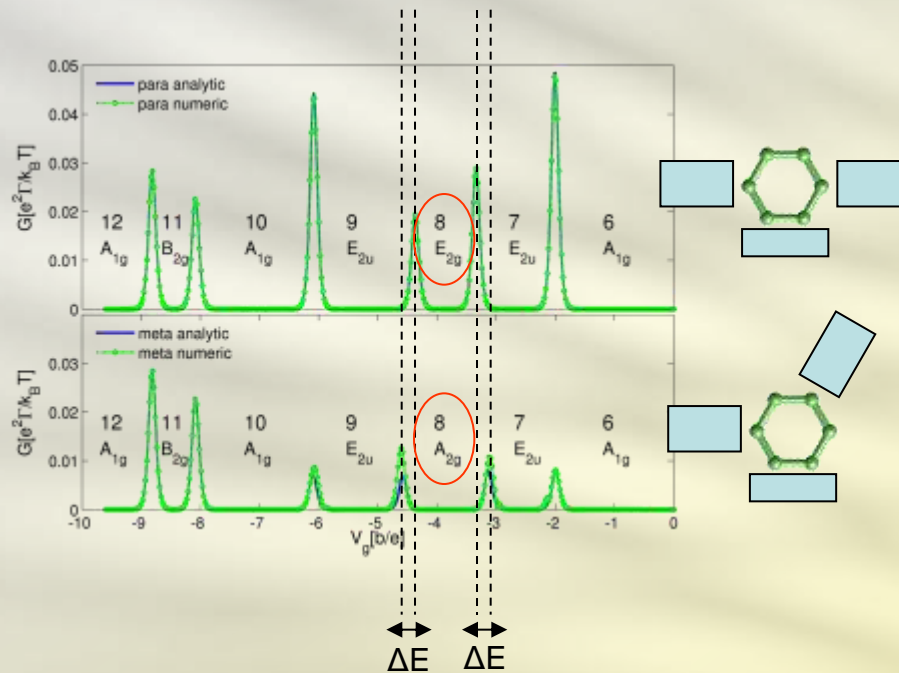


Interference Blockade

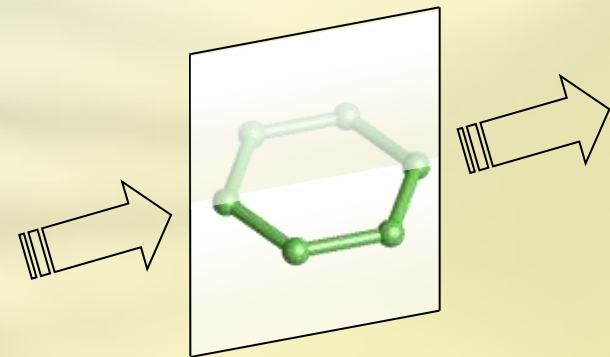


Three linear combinations of 2-particle excited states are coupled **ONLY to the source**.

The 8 electrons "anomaly"

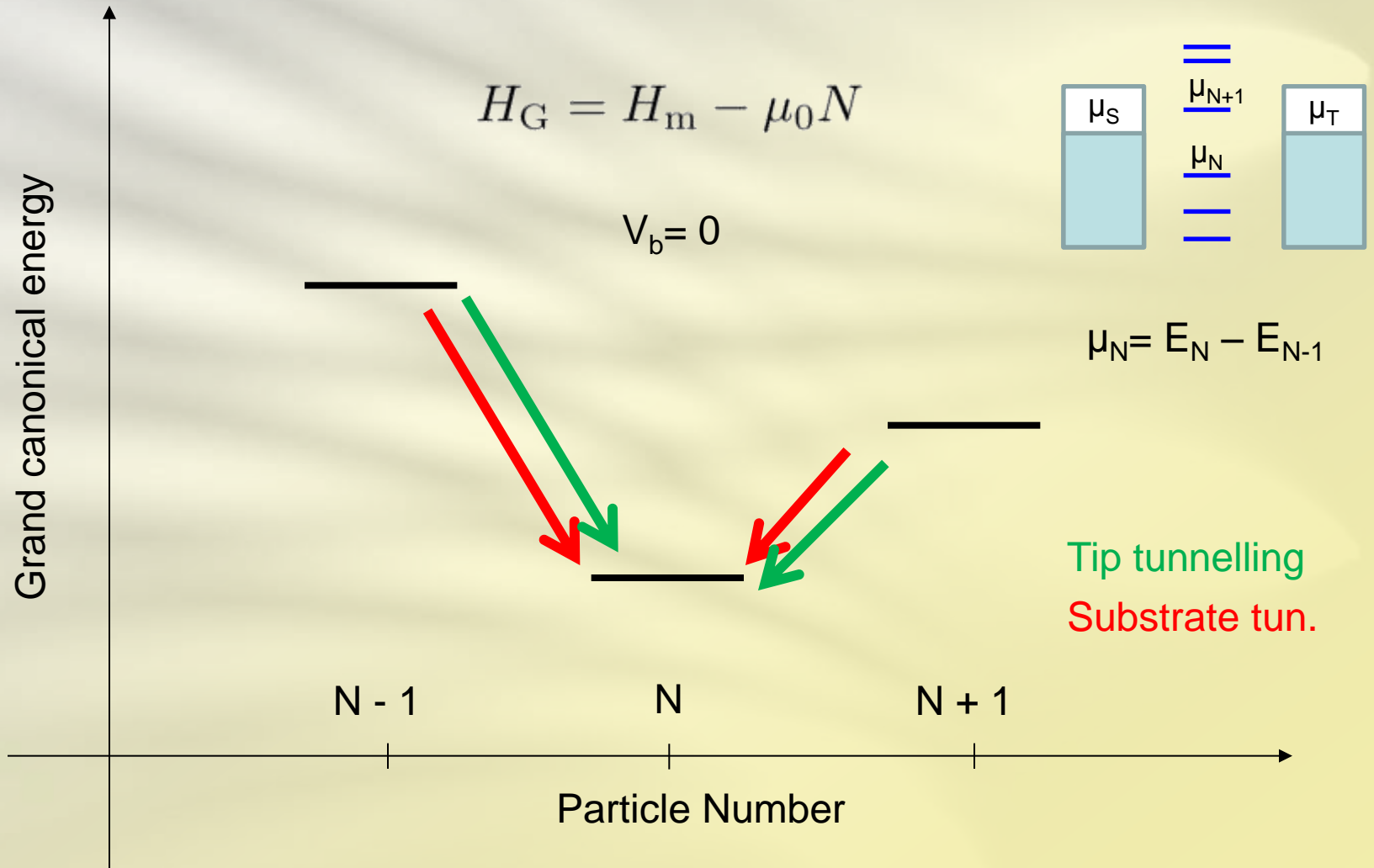


Mirror symmetry of the para-configuration

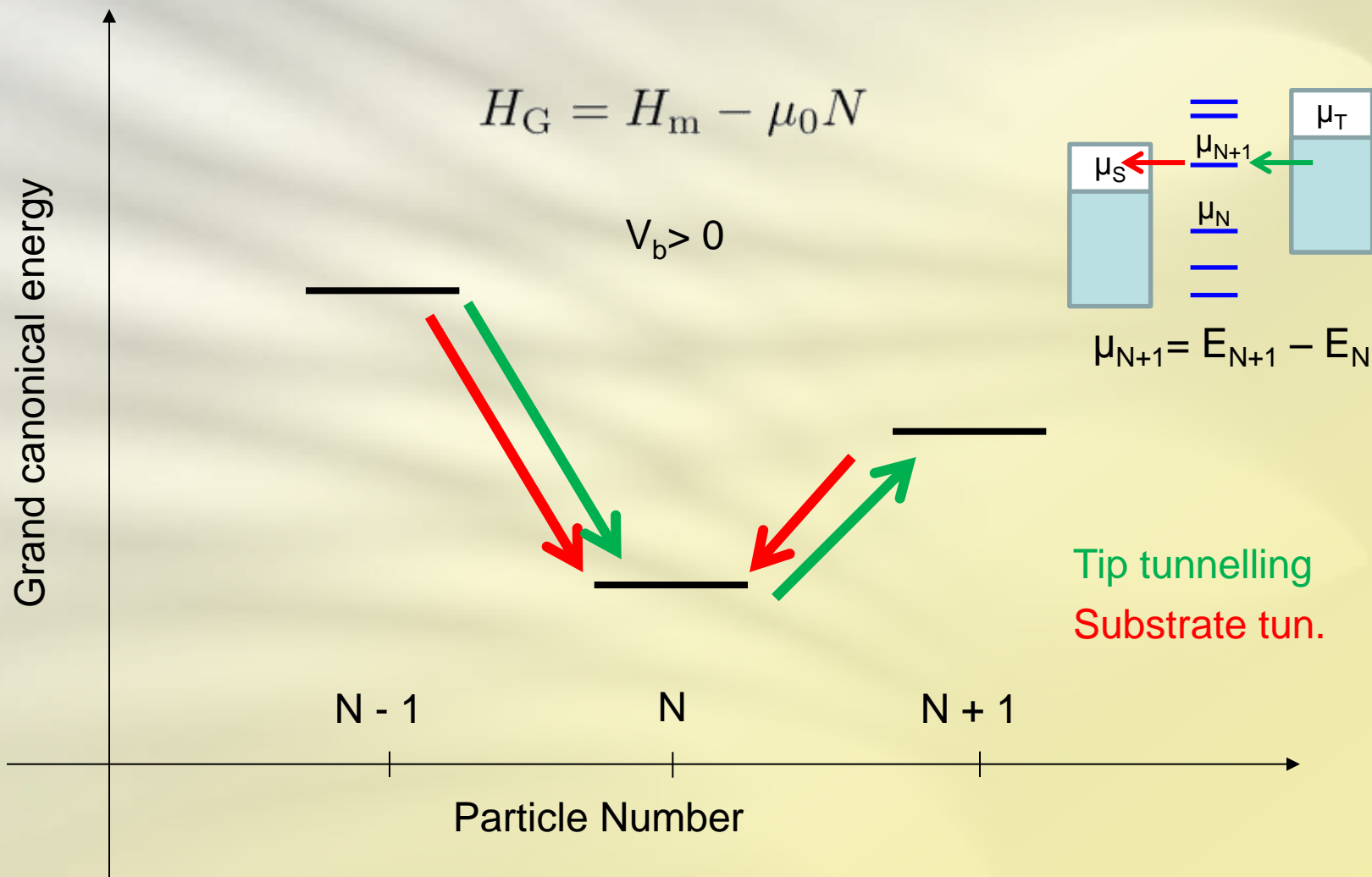


The tunnelling preserves this **mirror symmetry**: the lowest 8 electron state involved in transport is the mirror-symmetric (first excited) state with E_{2g} symmetry.

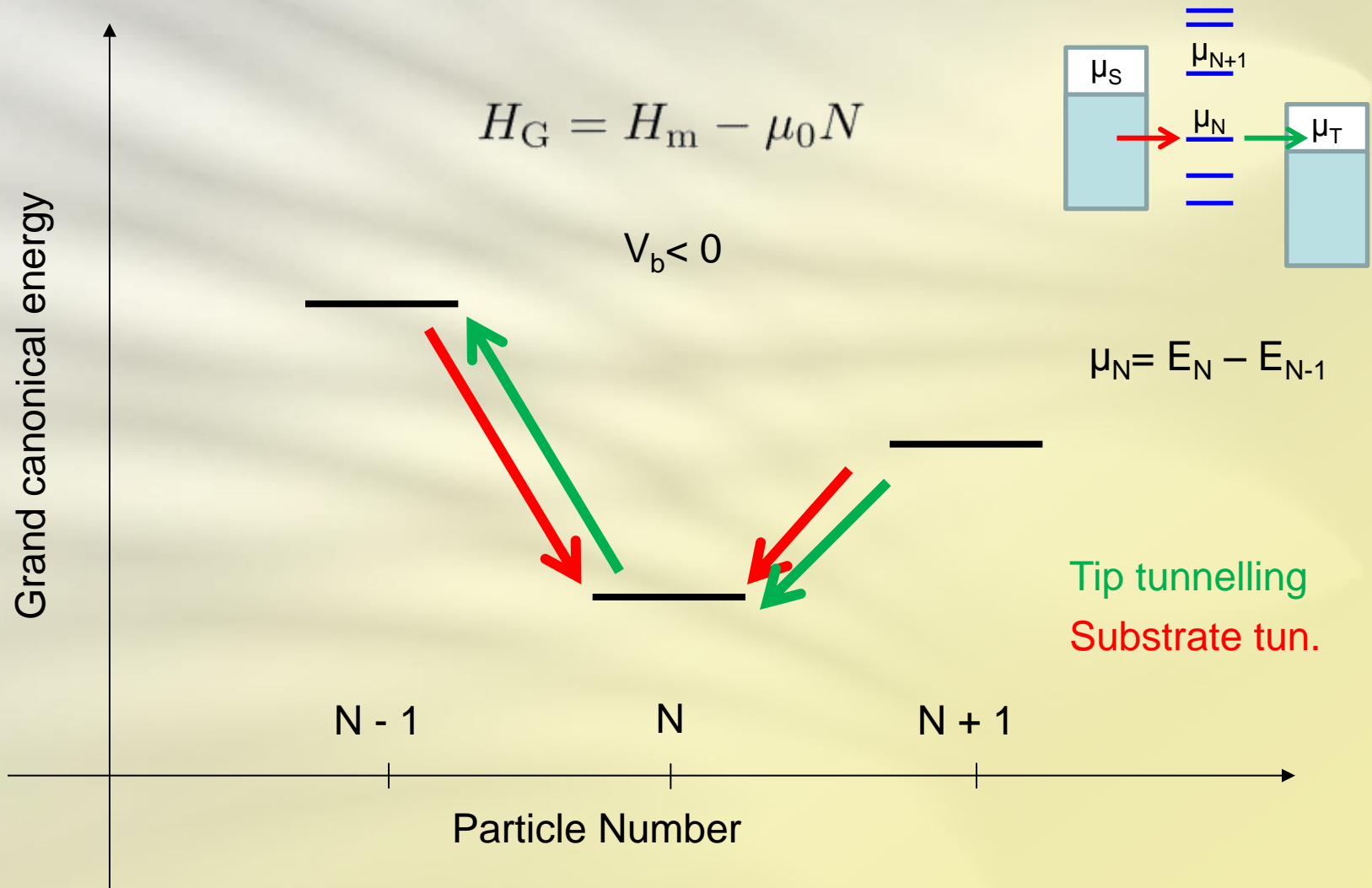
Dynamics in energy space



Dynamics in energy space

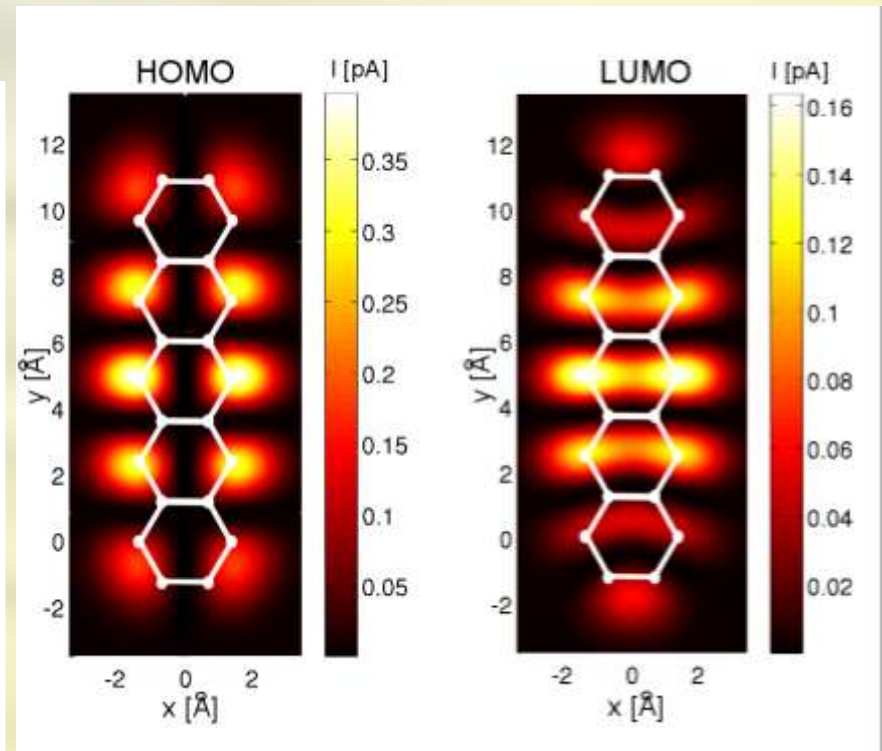
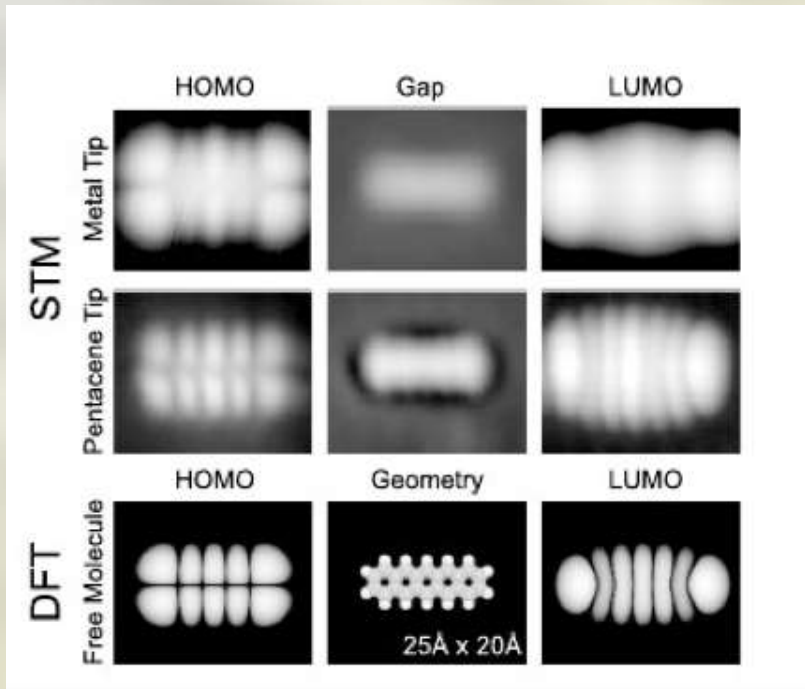


Dynamics in energy space



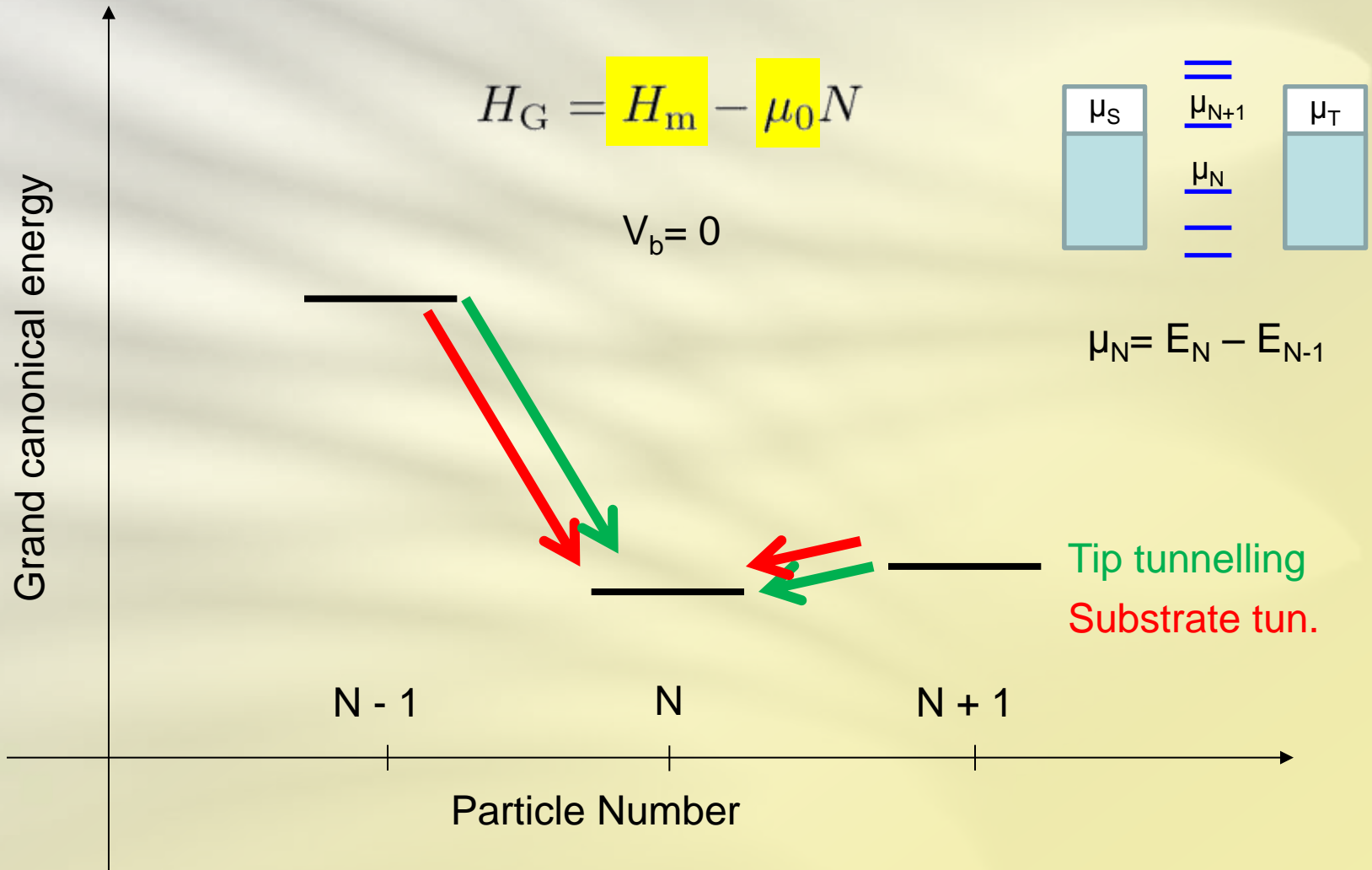
Visualization of molecular orbitals

Topography

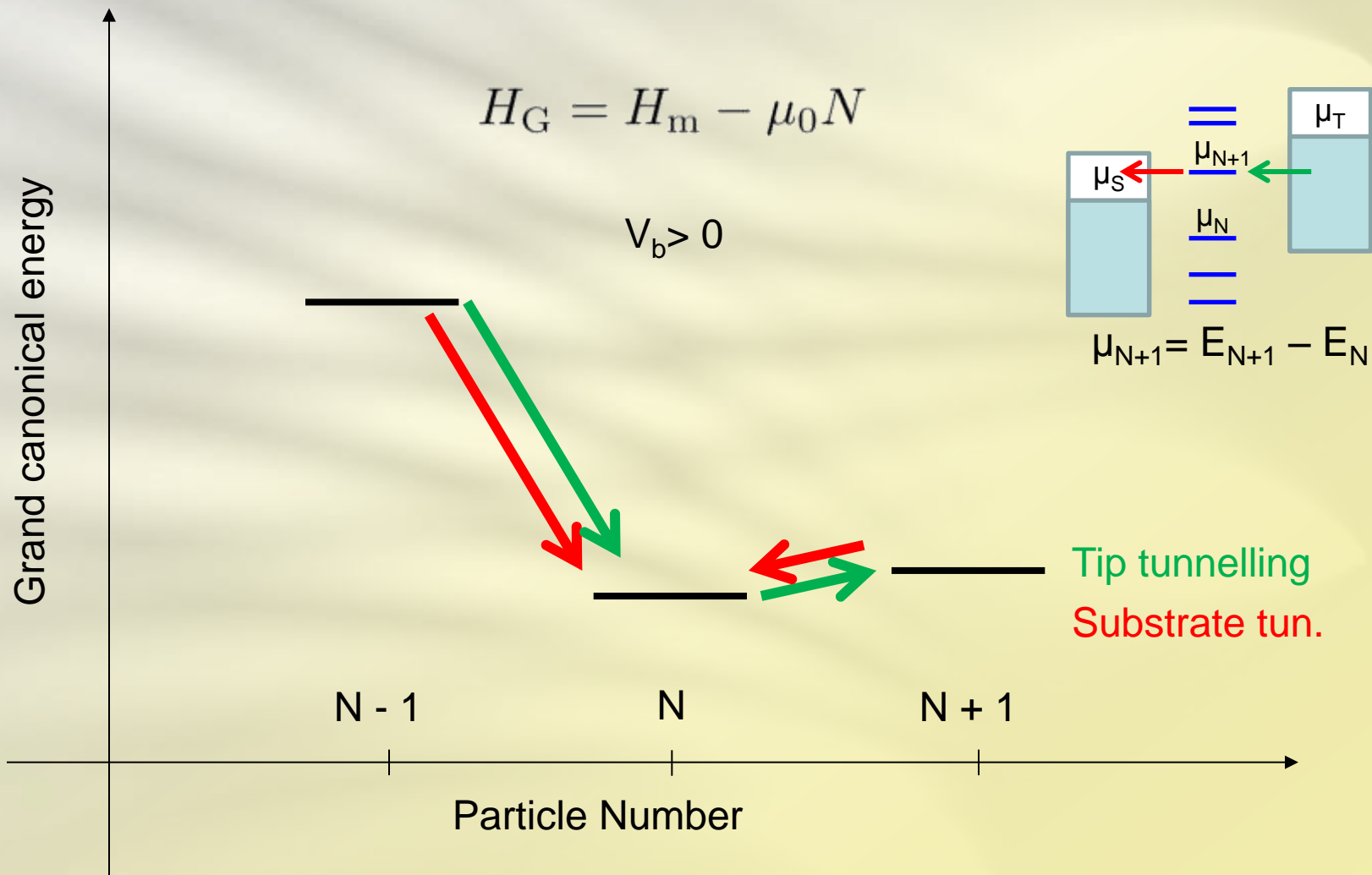


J. Repp and G. Meyer, Physical Review Letters **94**, 026803 (2005)

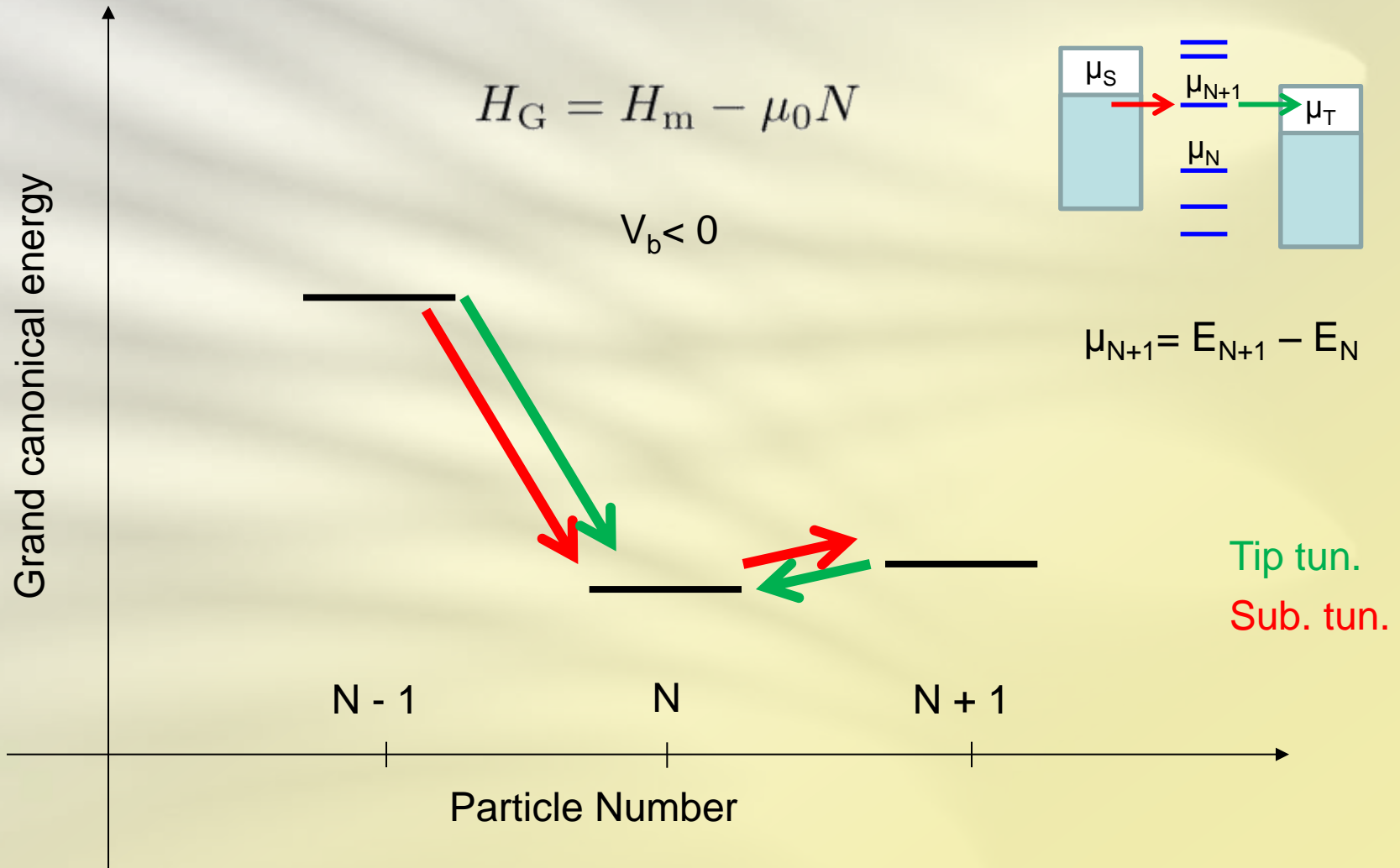
Dynamics in energy space



Dynamics in energy space



Dynamics in energy space



Robustness

- We have tested the **robustness** of the effects against:
 - Residual **potential drop** on the (artificial) molecule (in weak coupling to the leads the potential drop is concentrated at the contacts)
 - On-site **energy renormalization** of the contact atom due to different anchor groups
 - Lifting of the electronic degeneracy due to deformation (**static Jahn-Teller effect**)
- The minimal necessary condition is **quasi-degeneracy**:

$$\delta E \ll \hbar\Gamma$$

D. Darau, G. Begemann, **AD**, and M. Grifoni, *PRB*, **79**, 235404 (2009)

Blocking conditions

The interference blocking state:

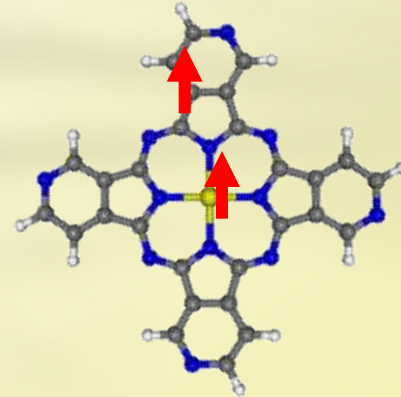
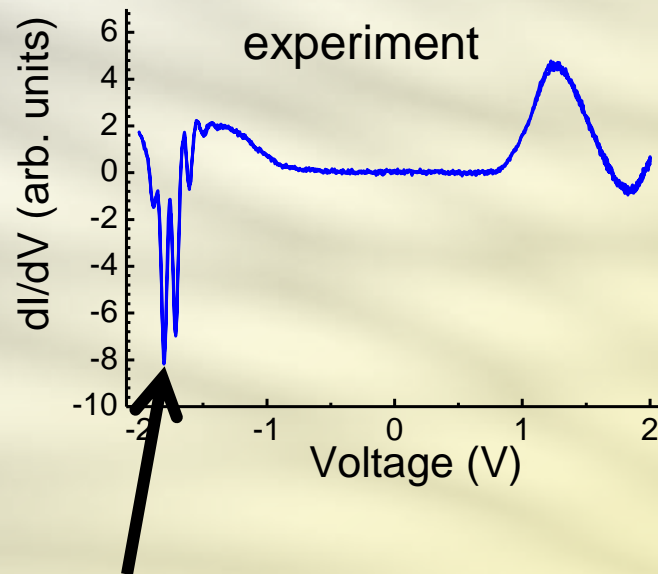
- is a **linear combination** of (quasi-)degenerate system eigenstates
- is **achievable from the global minimum** via a finite number of allowed transitions
- has **vanishing tunnelling amplitudes** for all energetically allowed outgoing transitions

$$\mathcal{L}_{\text{tun}}\sigma_B = 0$$

- is an eigenstate of the **effective Hamiltonian**

$$[H_{\text{eff}}, \sigma_B] = 0$$

Joint effort: Sources of Negative differential conductance



interference effect (?)
+ spin excitations
(exchange, spin-orbit coupling, ligand field, ...)